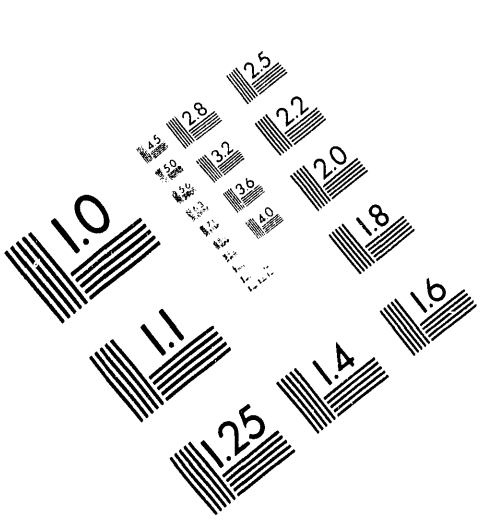

Association for Information and Image Management

1100 Wayne Avenue, Suite 1100
Silver Spring, Maryland 20910

301/587-8202

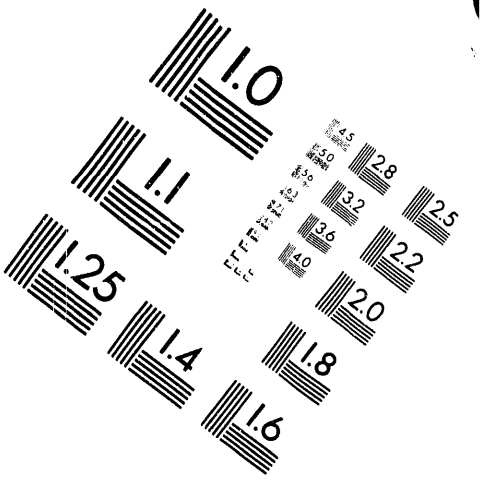

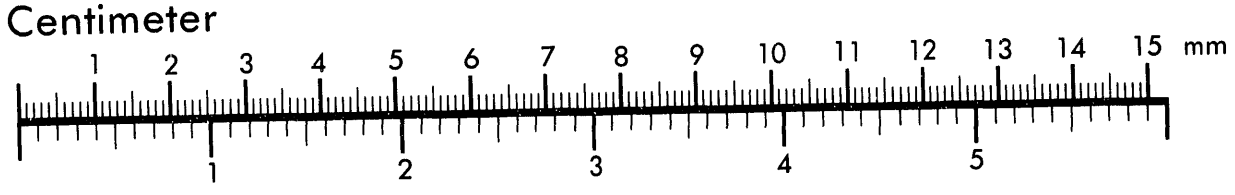

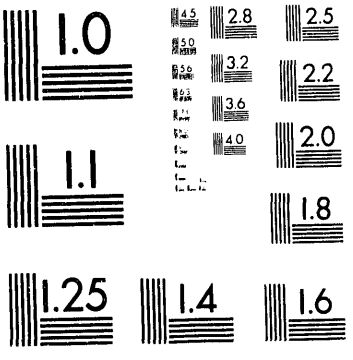

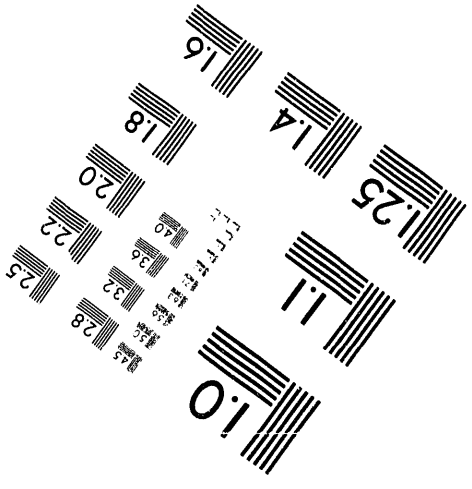

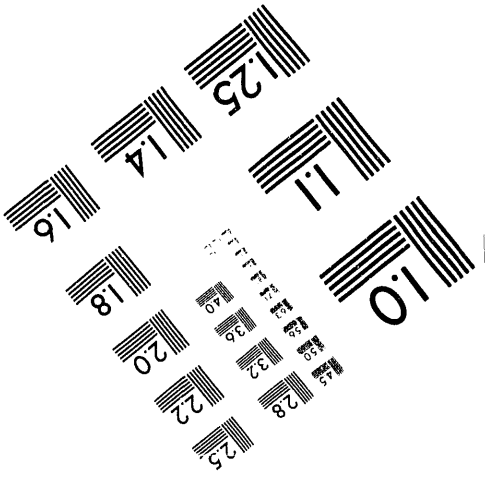

1 of 1

Final Report for DOE Grant

by

Catherine Goyet

Acknowledgments

This project has been supported by a grant from the U.S. Department of Energy. I thank Drs. Michael Riches and John Downing for their support and encouragement on this project. The field observations and sampling were conducted aboard the R/V *Thomas Washington*. I gratefully acknowledge the captain and the crew for their generous assistance provided during the cruise. This work would not have been possible without the scientific and technical assistance of Peter G. Brewer, Edward T. Peltzer, Alvin L. Bradshaw, and Sally D. Hacker.

Abstract

With the support from the Department of Energy, we participated in the World Ocean Circulation Experiment (WOCE) cruises to document the spatial variation of the properties of the carbonate system over the world ocean. With the other members of the DOE CO_2 science team, we took advantage of the initial postponed ship schedule to initiate an intercomparison of total dissolved inorganic carbon measurement in seawater. This work has proven to be essential for the measurements performed at sea soon after. We participated in 2 cruises in the Equatorial Pacific Ocean along 150° W and 135° W. Surface seawater CO_2 partial pressure (pCO_2) measured along 150° W has been compared with earlier measurements made by Ray Weiss in 1979 along the same cruise track. The large variations of surface seawater pCO_2 (pCO_2^{sea}) on short spatial and temporal scale do not allow us to determine whether anthropogenic CO_2 modified pCO_2^{sea} in this ocean area. In the laboratory we also investigated a different means of measuring total alkalinity by thermometry.

Introduction

The significant increase of anthropogenic CO_2 gas in the atmosphere affects the Earth's global climate. By continually exchanging heat and greenhouse gases with the atmosphere, the global ocean plays an important role in the regulation of the Earth's climate. The ocean contains about 50 times more carbon than the atmosphere and may potentially absorb all the anthropogenic CO_2. However, the kinetics of the CO_2 gas transfer across the ocean-atmosphere interface are very slow. The process of CO_2 gas exchange between the ocean and the atmosphere is controlled by the complex interactions of biological activities throughout the water column, the ocean chemical CO_2 buffer capacity, and the ocean circulation dynamics. The relative importance of these processes varies both spatially and temporally.

The atmospheric data suggest that only approximately 55% of the anthropogenic CO_2 gas injected into the atmosphere remains there. Most of the other 45% is thought to be taken up by the ocean. The atmospheric signal is now large, being equal to approximately a 70 µatm increase in pCO_2, corresponding to an increase of approximately 45 µmol/kg TCO_2 in modern surface waters and to an increase in ΔpCO_2 (difference between surface seawater pCO_2 and atmospheric pCO_2) of approximately 8 µatm. Yet, direct oceanic observations are incomplete to confirm this hypothesis.

The main difficulties in performing these oceanic observations are mainly attributed to the large spatial and temporal variation of surface pCO_2 and to the limited resources (shiptime and manpower) compared to the immensity of the ocean, rather than to the analytical procedures. It is currently possible to measure seawater pCO_2 with an accuracy close to 1 µatm, and seawater TCO_2 with an accuracy close to 1.5 µmol/kg. The amplitude of the spatial and temporal variations of pCO_2 can reach more than

140 µatm corresponding to more than 17 times the amplitude of the anthropogenic signal. The short term variability (<day) is close to 10 µatm. The seasonal and interannual variability of surface waters pCO_2 ranges from 8 µatm to more than 100 µatm.

In this highly variable ocean, several complementary approaches are now underway to detect the anthropogenic signal and predict future changes:

1) *Continual monitoring of the carbonate properties in the ocean.*
Survey and time-series shipboard measurements are currently performed within the JGOFS/WOCE programs. Additional time-series measurements are currently made regularly in 2 ocean areas close to Bermuda and Hawaii. Such monitoring should be expanded to other areas. New analytical procedures are now being developed to monitor surface water pCO_2 from unattended platforms such as buoys.

2) *Modeling and remote sensing.*
Efforts are being made to parameterize the current understanding of the process involved in the variation of surface water pCO_2 as a function of properties (such as T or chlorophyll) that can be remotely sensed. This will provide better monthly estimates of pCO_2 over the global ocean.

3) *Monitoring of atmospheric pCO_2 and pO_2.*
As Keeling and Shertz (1992) showed, atmospheric pCO_2 and pO_2 measurements can be used to estimate a global average of the transfer of anthropogenic CO_2 into the ocean.

In this report, we summarize the results of the at-sea measurements of the parameters of the carbonate system in seawater on the WOCE cruises P16c and P17c, as well as the theoretical and experimental results of laboratory studies made to improve the measurement techniques.

I) On-Shore Activities/Studies

1) We contributed to the DOE science team effort in the preparation of a handbook on the standard operating procedures for the measurements of the various parameters of the carbonate system in seawater. This DOE handbook (1991) is now widely distributed to the international scientific community, and is being updated as progresses are made.

2) We contributed to the progress of the technical measurement of C_T in seawater; we investigated a means of calibration of the coulometric system currently used for such C_T measurements (manuscript enclosed: Goyet and Hacker, 1992).

3) We contributed to the DOE sponsored interlaboratory comparison of total CO_2 (C_T) measurements exercise, by measuring C_T on reference material prepared by A. Dickson from Scripps. Using our calibration method mentioned in item 2, our results matched, within the standard error of the measurements, the data from C.D. Keeling's laboratory which were regarded as the reference data.

4) We contributed to the teaching of the measurement of C_T and A_T in seawater; N. Bates, from the Bermuda Biological Station (from March 11th through 15th, 1991), and D. Chipman, J. Goddard, D. Berger, S. Rubin and D. Archer, all from Lamont-Doherty Geological Observatory of Columbia University (on April 17th, 1991) came to our laboratory to become acquainted with our methods of measuring C_T and total alkalinity (A_T) in seawater.

5) We investigated a means of measuring total alkalinity in seawater by thermometry. See Appendix 1 for a complete discussion of this research.

6) We studied the variations of pCO_2 as a function of temperature. Since the discrete measurements of pCO_2 in seawater are performed at constant temperature, data from the surface seawater need to be corrected to the *in situ* temperature before one can estimate the CO_2 flux across the air-sea interface. We therefore theoretically and experimentally determine the variations of CO_2 fugacity in seawater (manuscript enclosed: Goyet *et al.*, in review).

7) We measured total alkalinity samples that were collected by Doug Wallace (from Brookhaven National Laboratory) during the WOCE cruise A9. The results of these measurements have been sent to Doug Wallace.

II) At-Sea Measurements

We participated in two WOCE cruises (P16c and P17c) in the Equatorial Pacific Ocean along 135° W and 150° W. The results of our measurements have been sent to CDIAC and will be quality controlled by the procedure the DOE CO_2 science team is currently investigating. Since the final hydrographic data for these cruises are not yet available, our data (that need the density of seawater samples) are still preliminary. The data will be available to the scientific community as soon as the hydrographic data set will be available to us and our data corrected for the density. Figs. 1 to 3 show the results of our measurements of total inorganic carbon and total alkalinity using the available preliminary hydrographic data.

The results of our pCO_2 measurements in seawater along 150° W have been described and compared with Ray Weiss' measurements performed in 1979 along the same cruise track (manuscript enclosed: Goyet and Peltzer, in press).

References:

DOE (1991). *Handbook of Methods for Analysis of the Various Parameters of the Carbon Dioxide System in Seawater*. A. G. Dickson and C. Goyet, eds.

Goyet, C. and S. D. Hacker (1992). Procedure for calibration of a coulometric system used for total inorganic carbon measurements in seawater. *Marine Chemistry*, **38**, 37-51.

Goyet, C. and E. T. Peltzer (in review). Comparison of the 1991 pCO_2 distribution in the Equatorial Pacific Ocean along 150°W with that measured in 1979. *Global Biogeochemical Cycles* (Submitted Nov. 1992).

Goyet, C. F. J. Millero, A. Poisson, and D. K. Shafer (in review). Temperature dependence of CO_2 partial pressure in seawater. *Marine Chemistry*.

Keeling, R. F., and S. R. Shertz (1992). Seasonal and interannual variations in atmospheric oxygen and implications for the global carbon cycle. *Nature*, **358**, 723-727.

DISCLAIMER

Figure 1

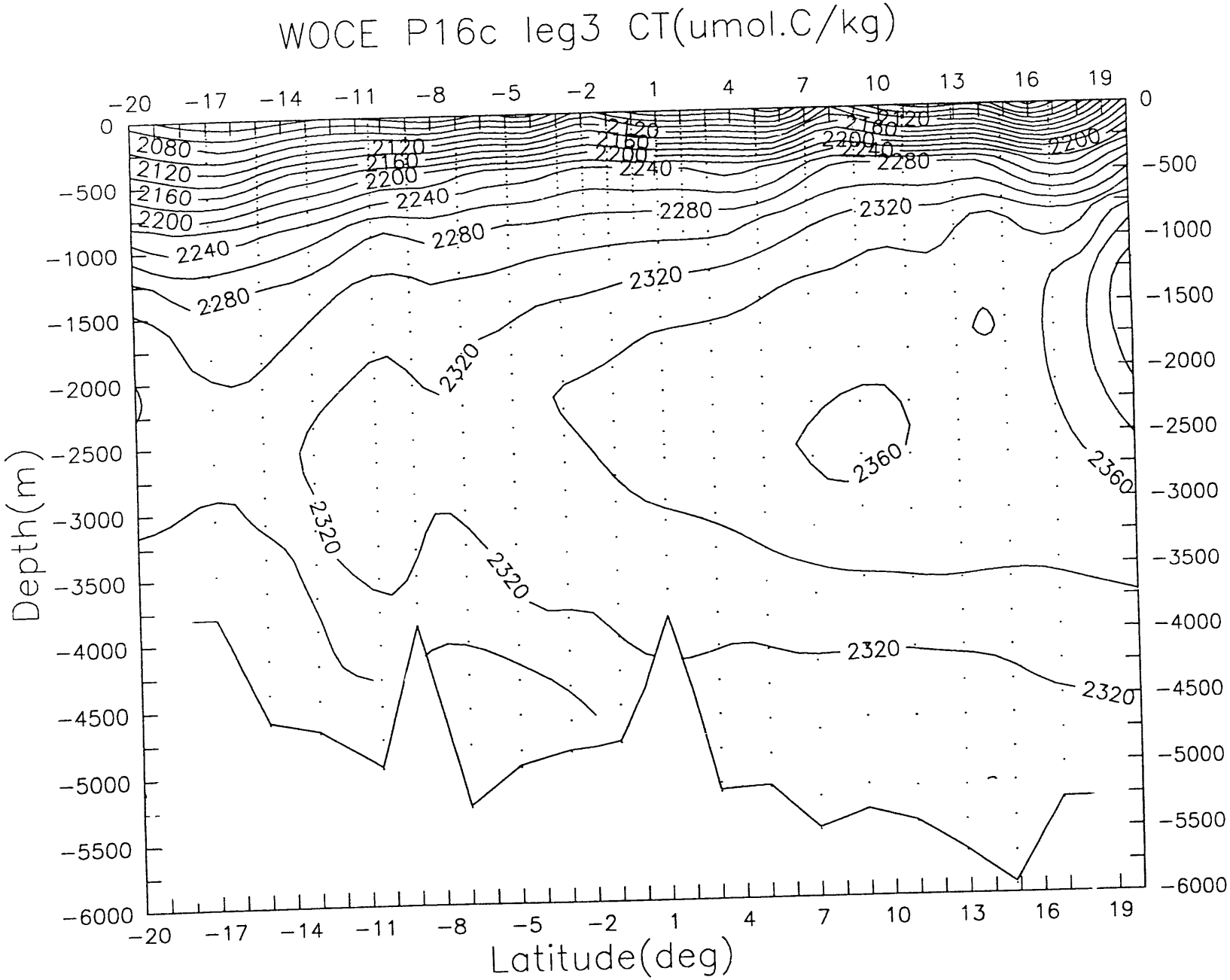
WOCE P16c leg3 CT(umol.C/kg)
Depth(m)
Latitude(deg)
-20 -17 -14 -11 -8 -5 -2 1 4 7 10 13 16 19
0 -500 -1000 -1500 -2000 -2500 -3000 -3500 -4000 -4500 -5000 -5500 -6000
2080
2120
2160
2200
2240
2280
2320
2360

Figure 2

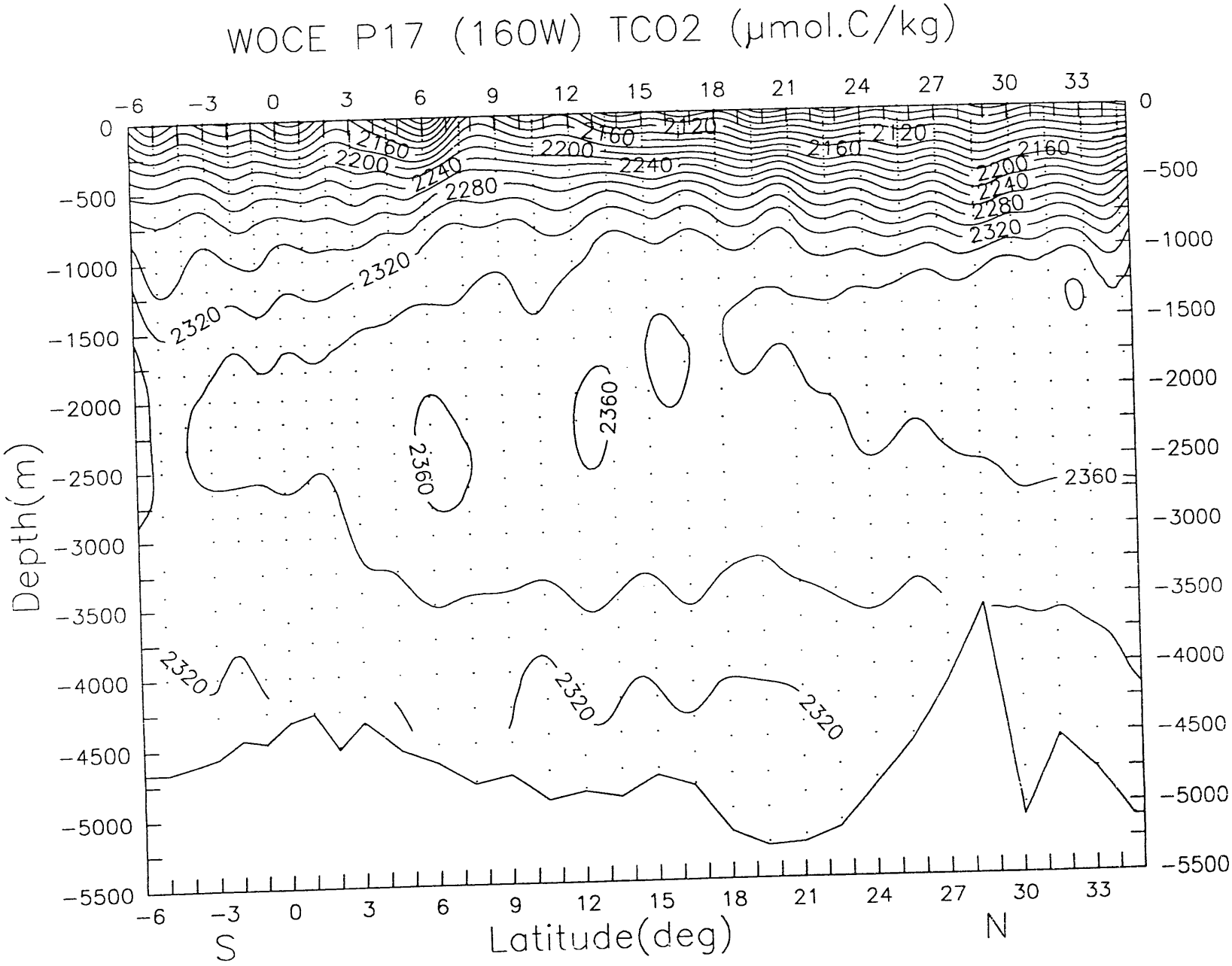
WOCE P17 (160W) TCO2 (μmol.C/kg)
Depth(m)
Latitude(deg)
S
N
2120
2160
2200
2240
2280
2320
2360

Figure 3

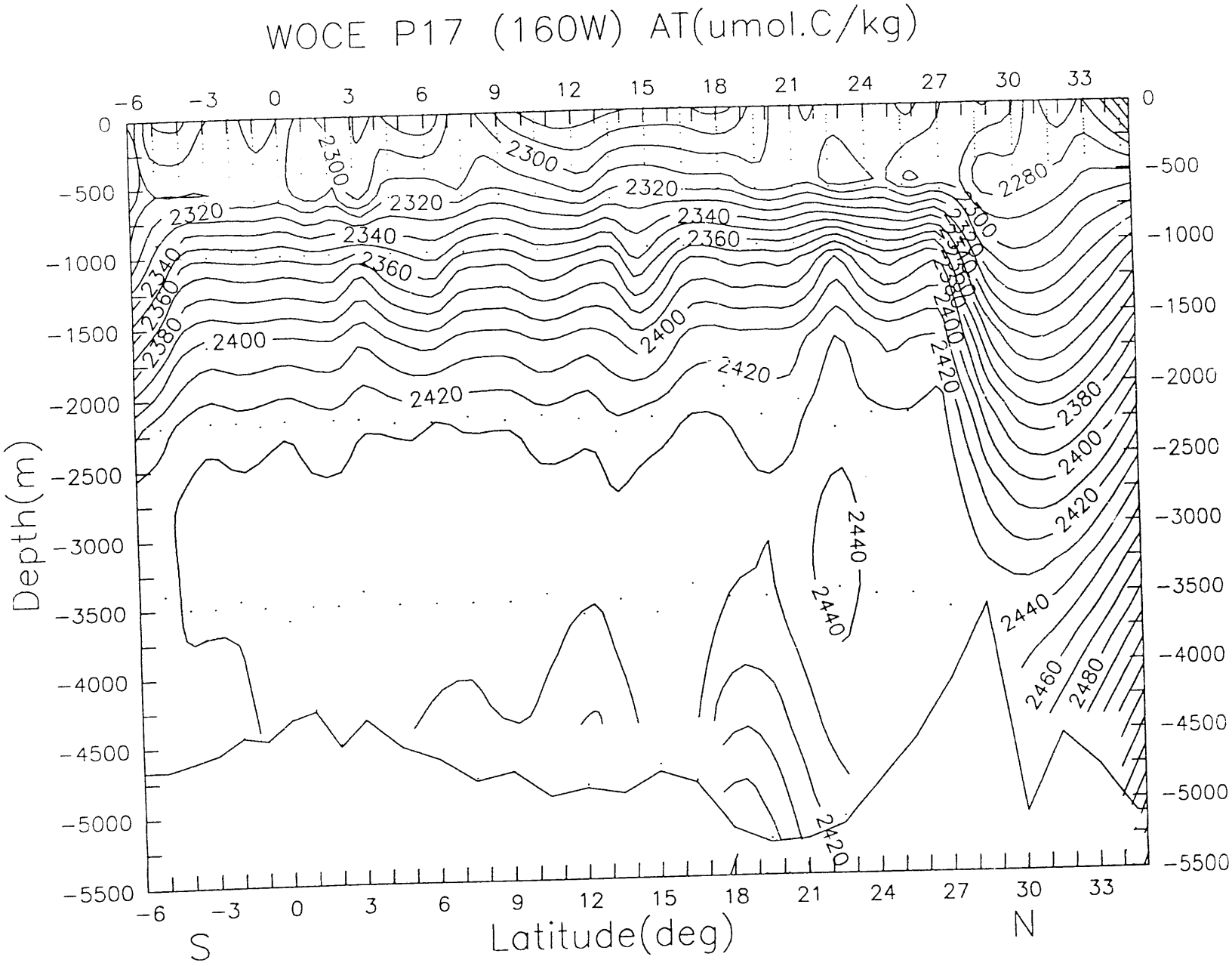
WOCE P17 (160W) AT(umol.C/kg)
Depth(m)
Latitude(deg)
S
N
-6 -3 0 3 6 9 12 15 18 21 24 27 30 33
0 -500 -1000 -1500 -2000 -2500 -3000 -3500 -4000 -4500 -5000 -5500
2300
2320
2340
2360
2380
2400
2420
2440
2460
2480
2280

Appendix 1: Thermometric Titration of Alkalinity

Compared to the conventional potentiometric titration, thermometric titration is potentially as precise but much faster (Millero *et al.*, 1974). However, since the determination of C_T by coulometry was not yet developed and since potentiometric titration was more precise for C_T than thermometric titration, the measurement of seawater samples for both C_T and A_T by thermometric titration was abandoned. Now that C_T can be measured accurately by coulometry, thermometric titration for A_T measurement alone presents several advantages. In particular, the simplicity of the system (which does not require a pH electrode) will simplify the calibration thus potentially improving both the accuracy and reliability of the measurement. The speed of the titration itself is approximately 10 times faster than that of the current measurements by potentiometry.

Apparatus

The apparatus consisted of a Tronac Isoperibol Titration Calorimeter (Model 458), a refrigerated bath/circulator as a source of cooling water for the cooled-heater water bath of the calorimeter, a Keithley 196 Digital Multimeter to measure the voltage unbalance of the calorimeter thermistor temperature bridge, and a Metrabyte MBC-488 General Purpose Instrument Bus (GPIB) Interface card to provide the interfacing between the DMM and a computer with an MS-DOS operating system. A block diagram of the system is shown in Figure 1.

As finally set up, we use a thermistor bridge sensitivity of 35 mv/°C and a temperature mv sampling rate of 1 per 0.12 sec. This sampling rate was obtained using no DMM digital filtering and no auto-calibration of the signal by introducing a FOR:NEXT loop of appropriate size into the data acquisition program (this rate can be increased to very slightly better than this). All of the titrations were carried out at 25°C in 50 ml sample dewar flasks provided by Tronac. We used an actual sample size of about 45 ml. The acid titrant chosen was a 0.15N $HClO_4$ solution containing 0.55N NaCl (to roughly approximate the composition and ionic strength of seawater samples).

Results

A sample thermogram is shown in Fig. 2a. In Fig. 2b, the same results are presented with the stirring heat and other non-reaction heats (estimated from a pre-reaction temperature vs. time sampling) removed. The negative slope in Fig. 2b occurring after the titration alkalinity reaction is completed is associated with the endothermic bisulfate formation reaction. The titration alkalinity reaction section of the thermogram can be divided into two parts, separated by the boric acid equivalence point. Between the boric acid equivalence point and one a short time before the reaction equivalence point (EP) the thermogram is fairly linear with time, as is also the section from a short time beyond EP. This linearity can be used in estimating EP from the intersection of the two straight line fits to these sections. The non-linearity between the beginning of the reaction (T_0) and EP causes some difficulty in determining T_0 accurately from the intersection of pre-reaction and reaction slopes.

To better study the problem of determining titration alkalinity accurately from thermometric results, a computer model for the thermometric titration was made. This was done by modifying an existing model program for potentiometric titration of alkalinity. The heats of reaction required in this modification were obtained 1) from Millero's fit of the Hansson constants involved and 2) from the empirical equations for the dissociation constants of the bisulfate ion and HF in seawater given by (Unesco, 1987; Dickson and Ridley, 1979), using the thermodynamic relationship $\Delta H_i = RT^2(\partial \ln K_i/\partial T)$, where ΔH_i is the heat of reaction of component *i*, R = gas constant, T = absolute temperature and K_i = dissociation constant. The stirrer heating, etc. found in the experimental thermograms was used in the model. A "theoretical" thermogram for approximately the same conditions as those for Fig. 2 is shown in Fig. 3a. The thermogram with pre-reaction temperature change removed is shown in Fig. 3b. The same results with a temperature noise corresponding to that found experimentally (s.d. = 1×10^{-3} mv) added were also generated. As an aid to the chemical reactions occurring, the concentrations of the components during the titration are shown in Fig. 4.

We have created two computer programs to analyze thermograms for T_0 and EP. The first finds each point from the intersection of straight lines fitted to segments of the thermogram before and after the point. An example of the fittings to a theoretical curve for S = 35, TA = 2200 μE/kg, TCO_2 = 2000 μM/kg and a typical noise value of 1×10^{-3} mv is shown in Fig. 6a for EP and in Fig. 6b for T_0. In this example the segments are for 0.5 min. intervals both 0.25 min removed from the estimated value of the point. "Convergence" to a final value is achieved by using each intersection value as the next guess. The values found for T_0 and EP are 0.91251 (σ =

0.0025) and 2.6832 (σ = 0.0020), in minutes. The true values were 1 and 2.6877 minutes, giving errors which are 5.2% and 0.3%, respectively, of the reaction time. The error in EP can be reduced to an acceptable value by standardizing against a known solution. The error in T_0 can be reduced to 0.4% of the reaction interval by using 0.1 minute segments 0.05 minutes removed from the estimated value of the point (Figure 6c). T_0 can also be located by eye in a magnified view, but in some cases this can be a too subjective method.

A second method of locating T_0 and EP is by looking at the first and second (difference) derivatives of the data. Both points are easily locatable in the theoretical model without noise (Figs. 7a, 7b, 7c, 7d). In the theoretical model with noise (Figs. 8a-8e), T_0 appears to be easily locatable in the plot of first derivatives, but obscured in the plot of second derivatives for low degrees of smoothing. Smoothing was done using the routine "smooft" from Numerical Recipes in C by Press *et al.* (Cambridge University Press, 1990). With greater degrees of smoothing, EP also appears in the plot of second derivatives but with a loss of sharpness. The same comments apply to the experimental results (Fig. 9a-9d) except that T_0 does not have the sharpness and certitude of that in the mathematical model and EP does not appear at all.

Because of the uncertainty in T_0 due to the curvature of the first part of the reaction interval, we decided to add a sufficient amount of acid to the sample before the titration in order to bring the sample solution into the linear portion of the reaction interval. Then T_0, as well as EP, could be found more accurately from the intersection of before and after straight-line fits. If the pre-titration acid addition is determined accurately, then the alkalinity of the original sample can be determined. Thermograms for this acid pre-addition method are shown in Figs. 10a-12d.

The escape of CO_2 from the solution could possibly bring the solution back into the curvature region. This was checked by measuring the pH of the solution at the beginning and at the end of the titration and does not appear to be the case.

Results for thermometric titration of a seawater of ~35 salinity are given in Table 1. EP was located by the intersection of straight line fits using 0.5 minute segments 0.25 minutes removed from the estimated value of the point; T_0 was found by using 0.1 minute segments 0.05 minutes removed from its estimated value. Results for thermometric titration of a seawater of S = 36.1 by the acid pre-addition method are shown in Table 2. In the case of EP 0.5 minute segments 0.25 minutes removed from the point were used; in the case of T_0 approximately 0.4 minute segments 0.05–0.1 minutes removed from T_0 were used.

Conclusions

Although it is not expected that thermometric titration for alkalinity will give as great an accuracy as the potentiometric method, the present results appear encouraging. A goal of 0.3% precision appears possible; such a precision would be a useful check in potentiometric results.

References

Millero, F. J., S. R.. Schrager, and L. D. Hansen (1974). Thermometric titration analysis of seawater for chlorinity, sulfate, and alkalinity. *Limnology and Oceanography*, **19**, 711-715.

Dickson, A. G. and J. P. Ridley (1979). The estimation of acid dissociation constants in seawater media from potentiometric titration with strong base. *Marine Chemistry*, **7**, 89-99.

Unesco/SCOR/ICES/IAPSO Joint Panel (1987). Progress on oceanographic tables and standards 1983-1986.

TABLE 1

Sample*	Alkalinity (μE/kg)+	
NS10	2198	
NS11	2210	
NS12	2201	
NS13	2158	Ave. = 2194
NS14	2203	sd = 19.6 (0.9%)
NS15	2177	
NS16	2212	Ave. with NS13 and NS15 omitted = 2205 and s.d. = 6.0 (0.3%)

* All samples except NS10 were weighed. Because NS10 had the same volume as the others (measured with a 50 ml syringe), its mass was taken as the average (s.d. = 0.3%).

+ The acid was not standardized – its prepared value (0.15N) was used.

TABLE 2

Sample	Mass Sample (g)	Acid Addition (g)	Acid Addition (sec)	Total Reaction Time (sec)	Total Reaction Time Adjusted to 45.62g Samples	Alkalinity* (μE/kg)
MILLSW3	45.46	0.1882	27.35	105.9_7	106.3_4	2377
MILL5	45.62	0.2027	29.45	106.7_1	106.7_1	2385
MILL6	45.62	0.2046	29.73	106.4_1	106.4_1	2379
					Ave = 106.4_8 sec s.d. = 0.20 (0.18%)	Ave. = 2380 μE/kg s.d. = 4.2 μE/kg

* The potentiometric titration value for titration alkalinity was assumed for MILLSW3 in order to show the scatter in μE/kg.

Figure 1

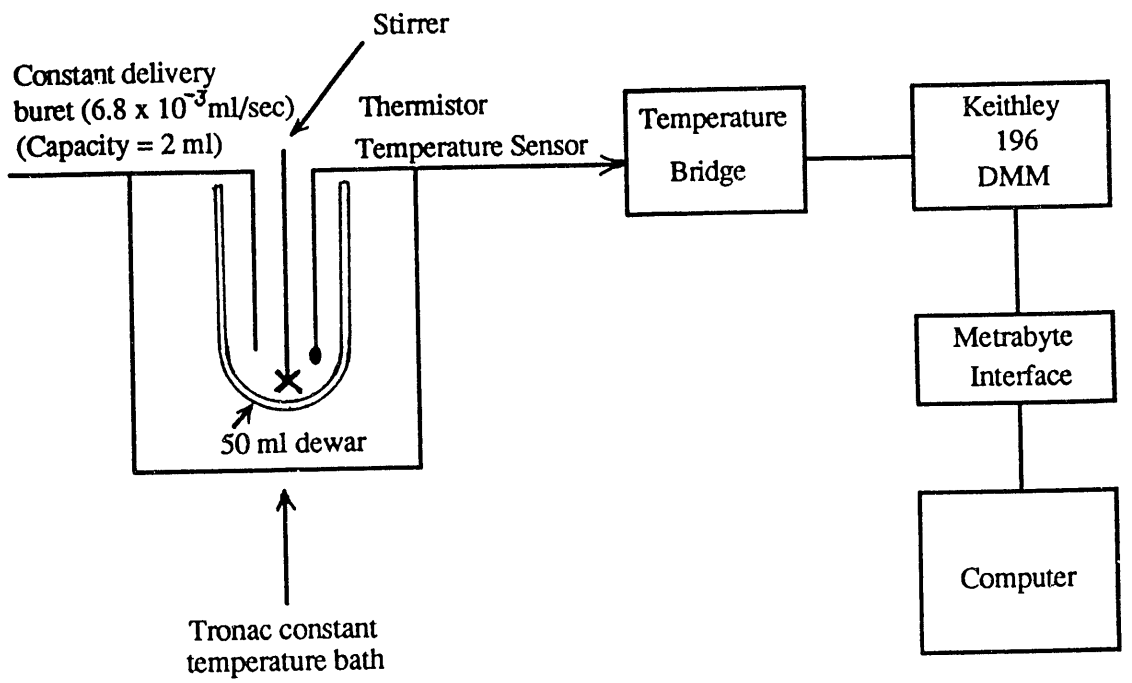
Stirrer
Constant delivery
buret (6.8 x 10^{-3}ml/sec)
(Capacity = 2 ml)
Thermistor
Temperature Sensor
Temperature
Bridge
Keithley
196
DMM
Metrabyte
Interface
Computer
50 ml dewar
Tronac constant
temperature bath

Figure 2a

Thermogram for Sample NS11

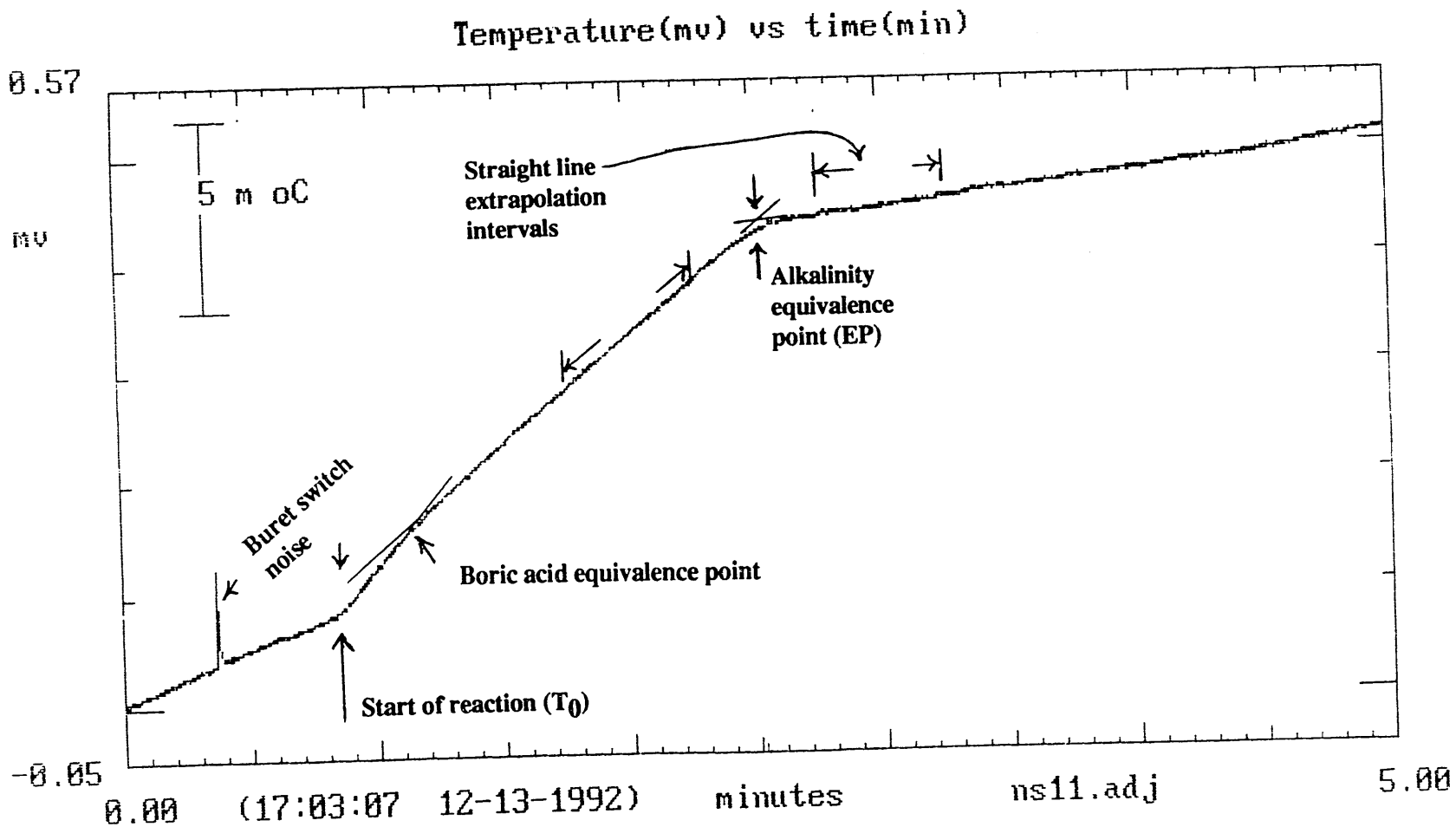

Figure 2b

Thermogram For NS11 With The Pre-Reaction Slope Subracted

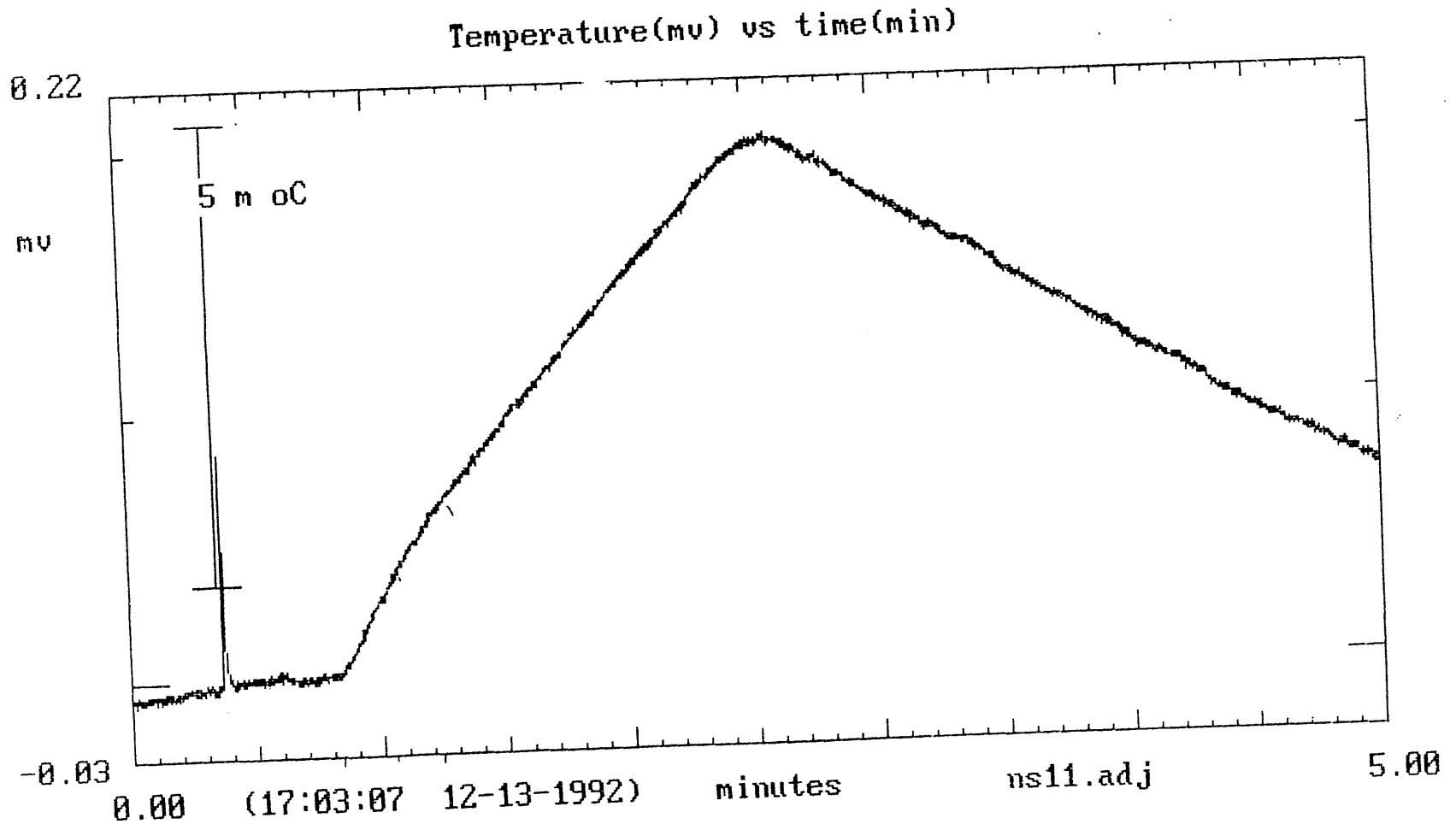

Figure 3a

Theoretical Thermogram For Experimental Conditions Of Figure 2

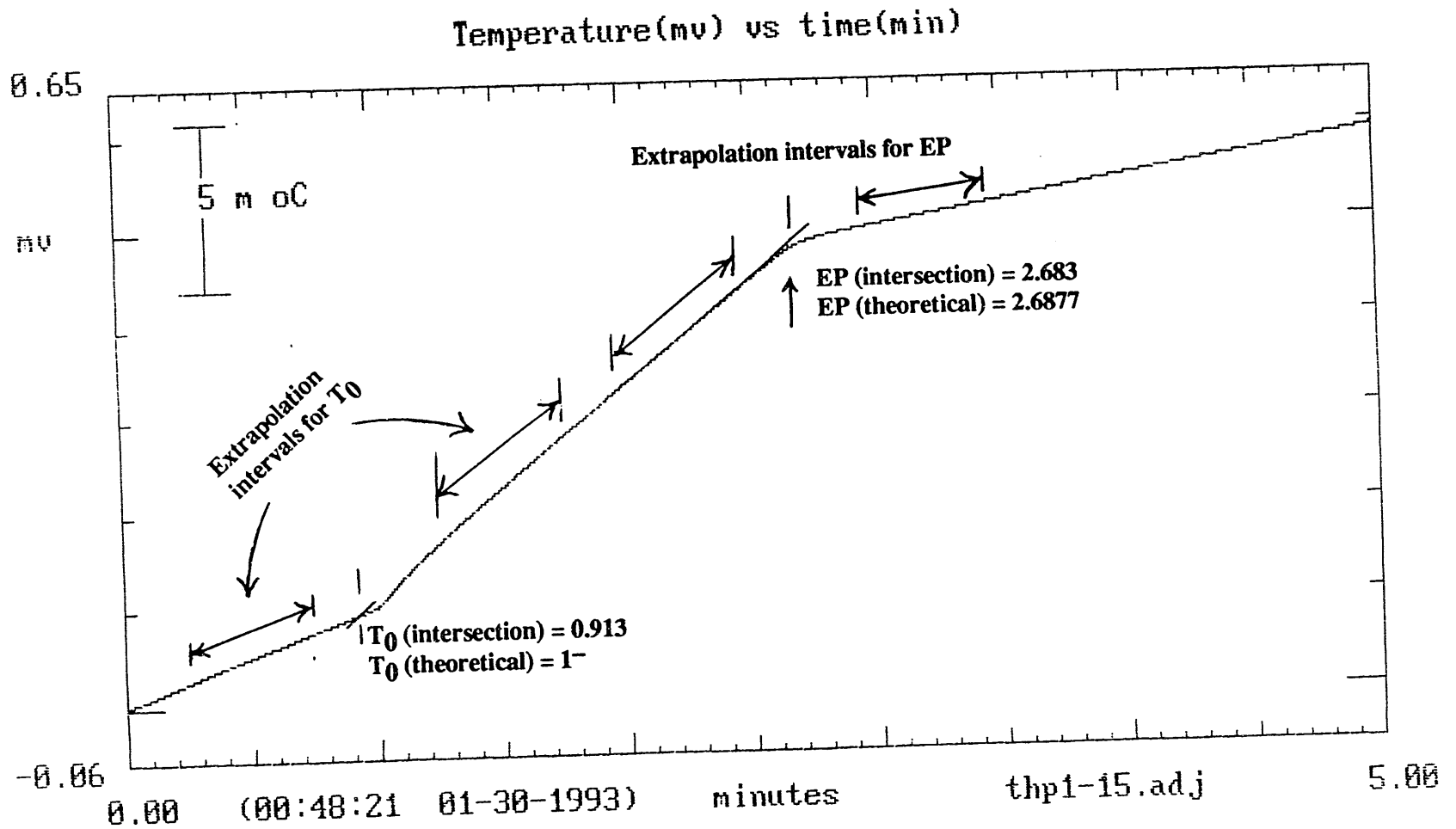

Figure 3b

Theoretical Thermogram With The Pre-Reaction Slope Subracted

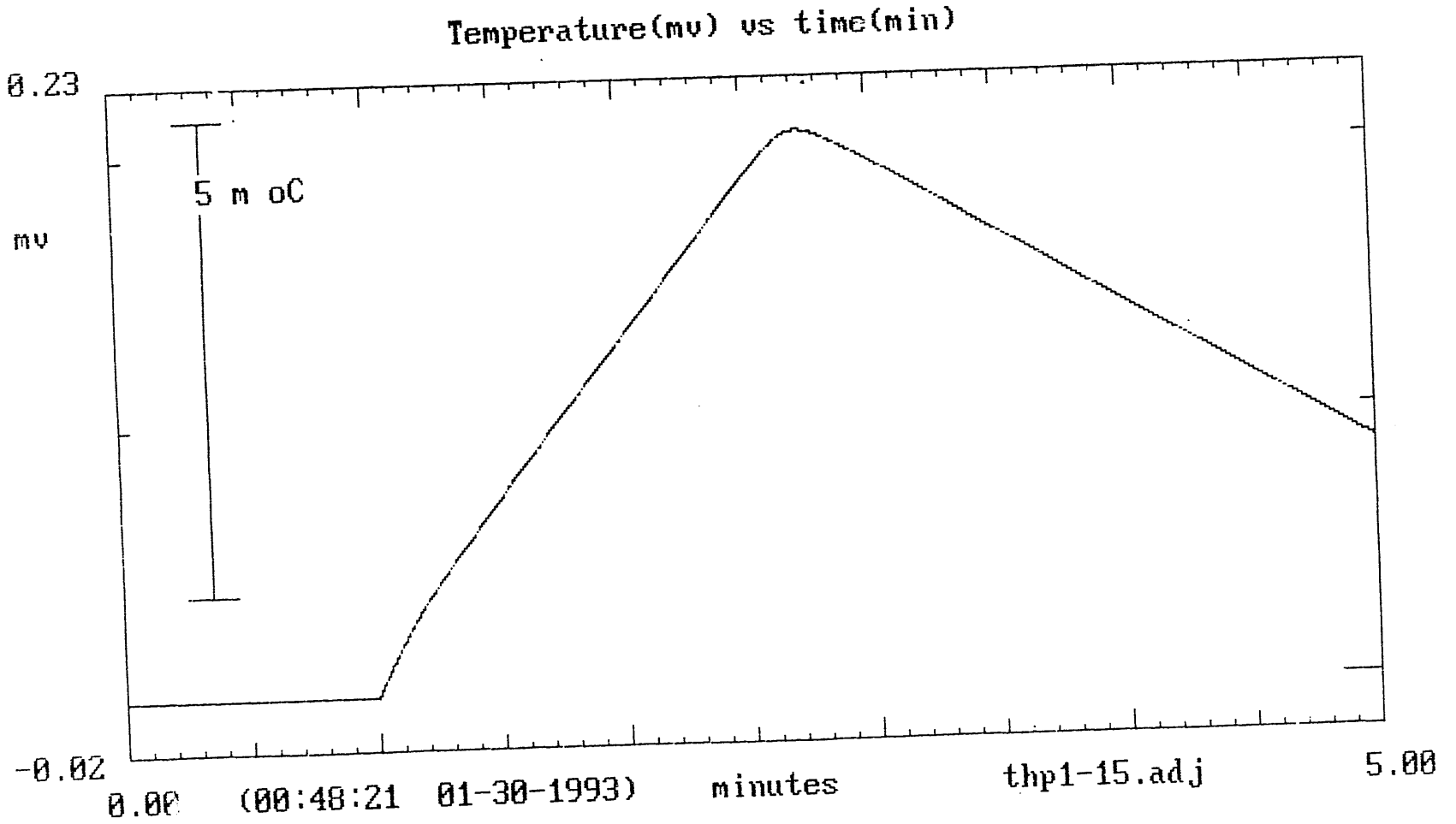

Figure 4

Concentrations For The Theoretical Titration Of Figure 3

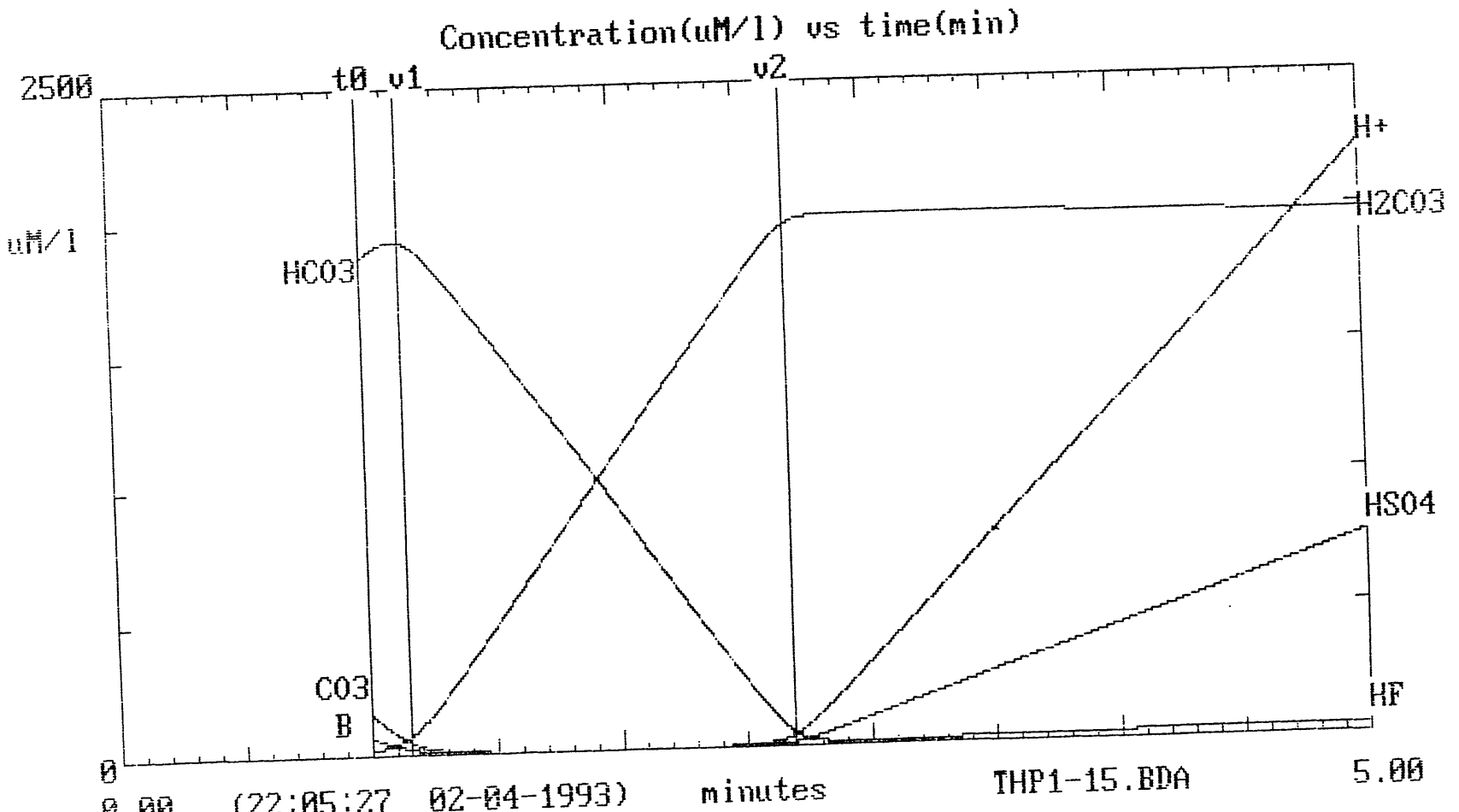

(A = 2200 µE/kg, TC = 2000 µM/kg, S = 35)

Figure 5a

Location Of T_0 On Theoretical Thermogram

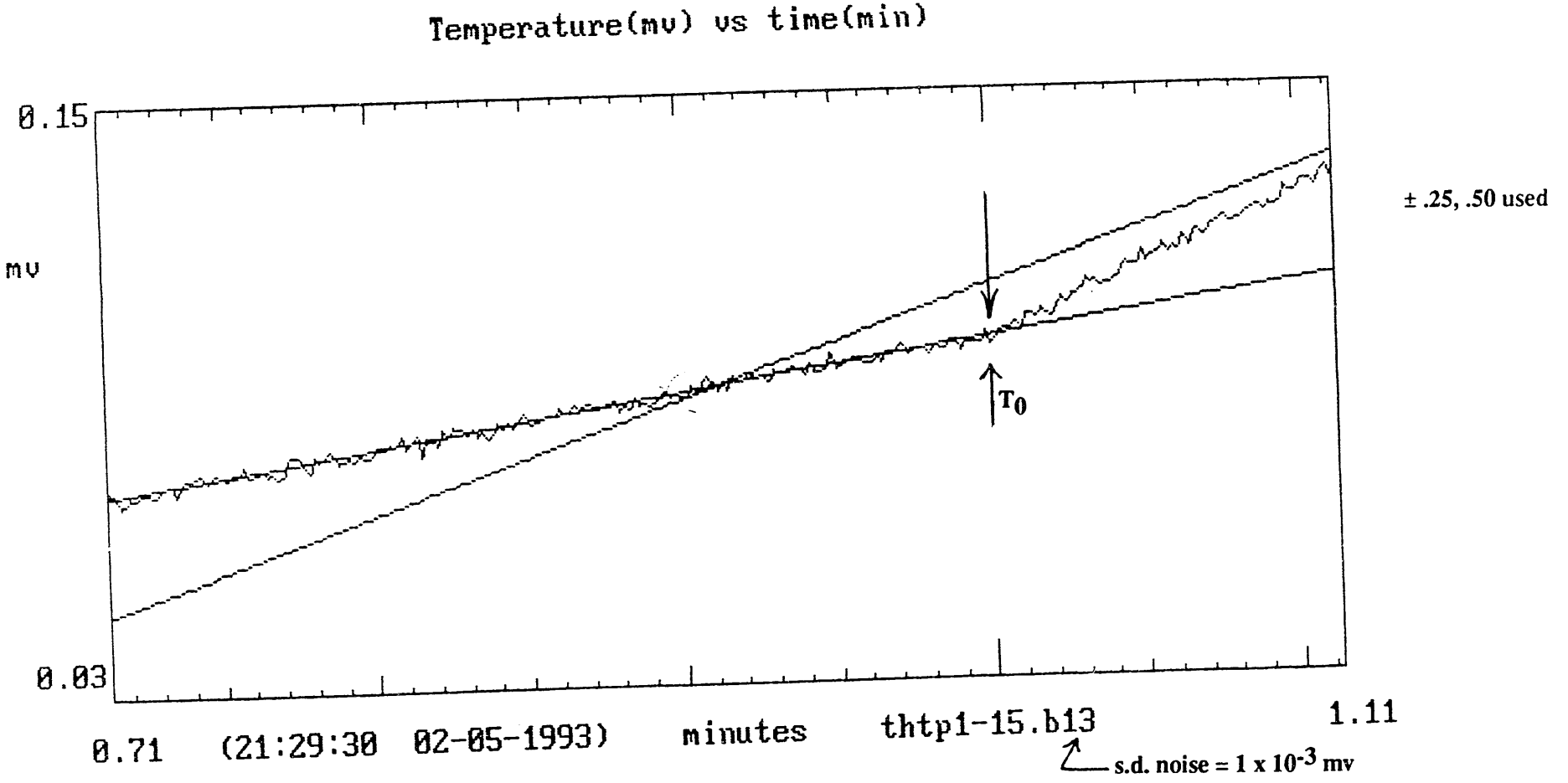

Figure 5b

Location Of EP Theoretical Thermogram

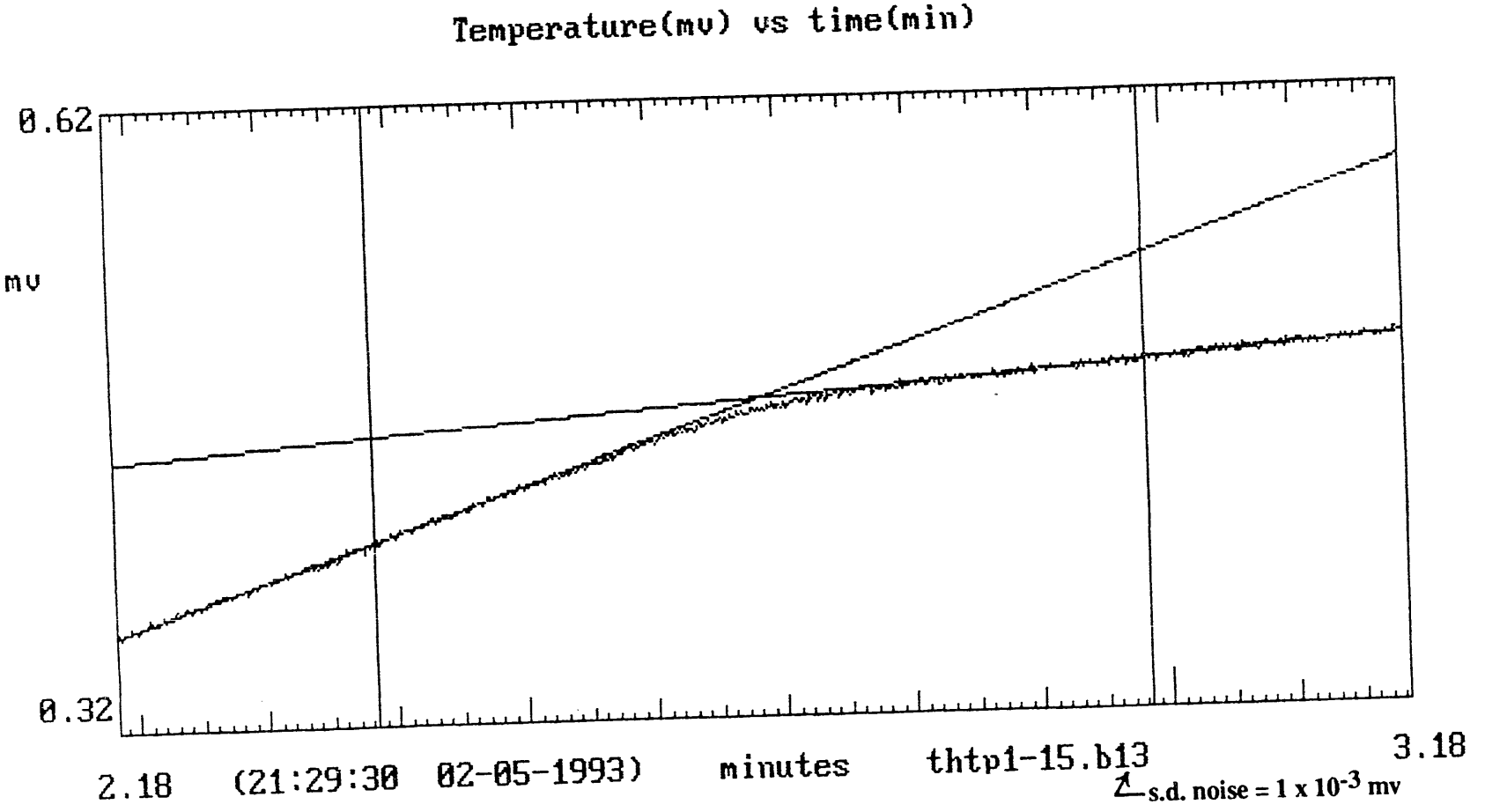

Figure 6a

Theoretical Model Without Noise

$$\frac{\delta(mv)}{\delta t}$$

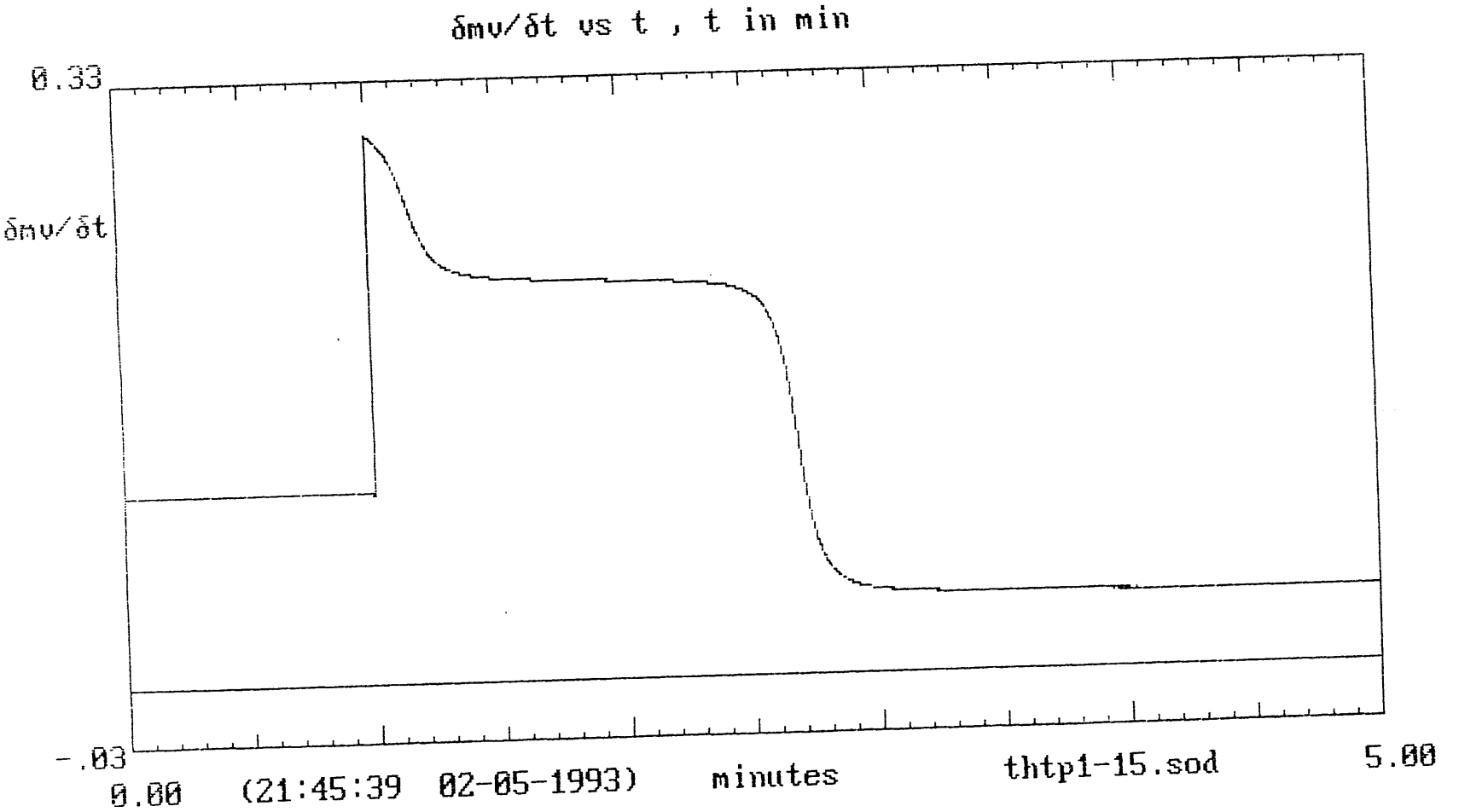

Figure 6b

Theoretical Model Without Noise

$$\frac{\delta^2(mv)}{\delta t^2}$$

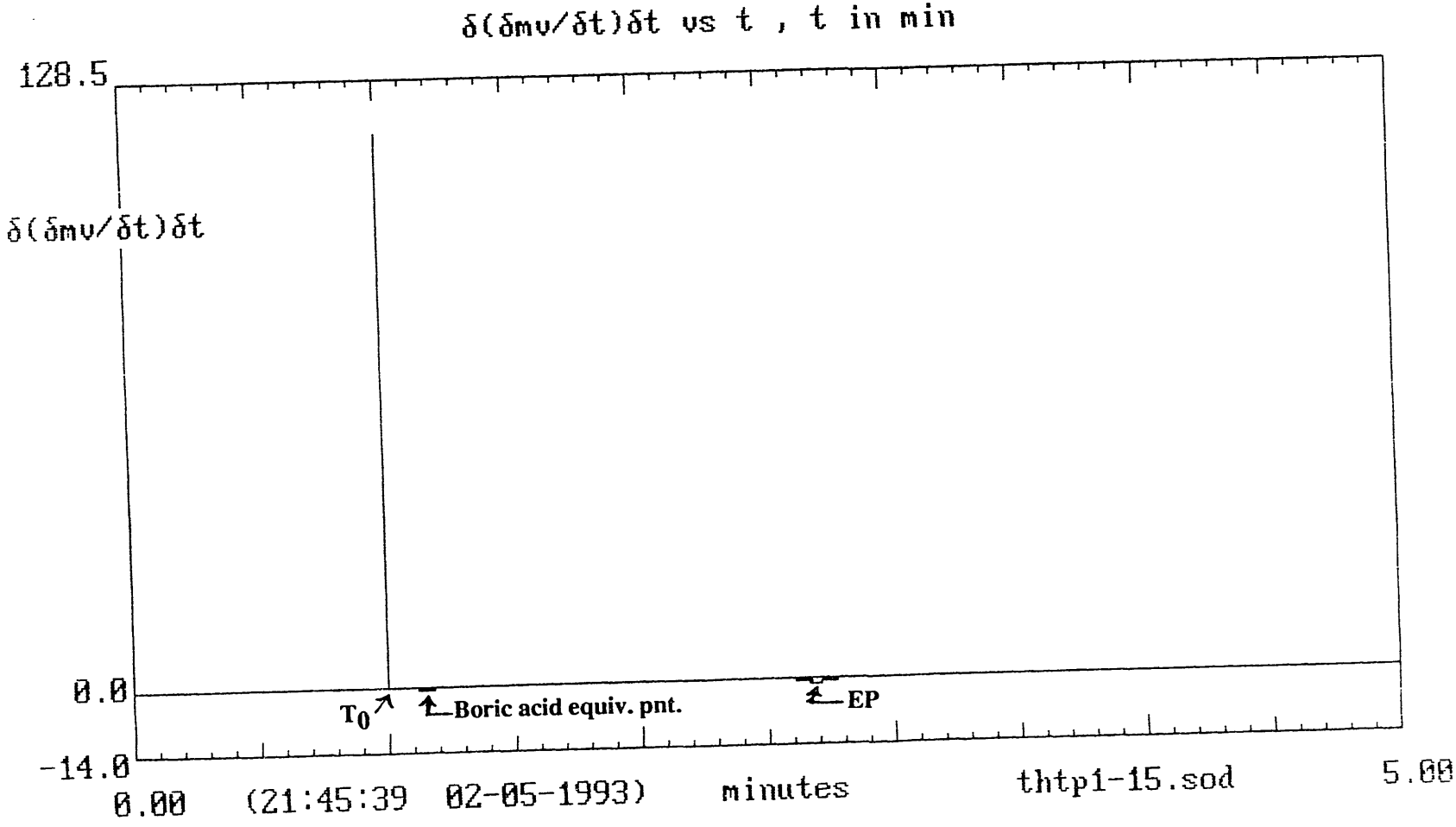

Figure 6c

Theoretical Model – Expanded Scale

$$\frac{\delta(mv)}{\delta t}$$

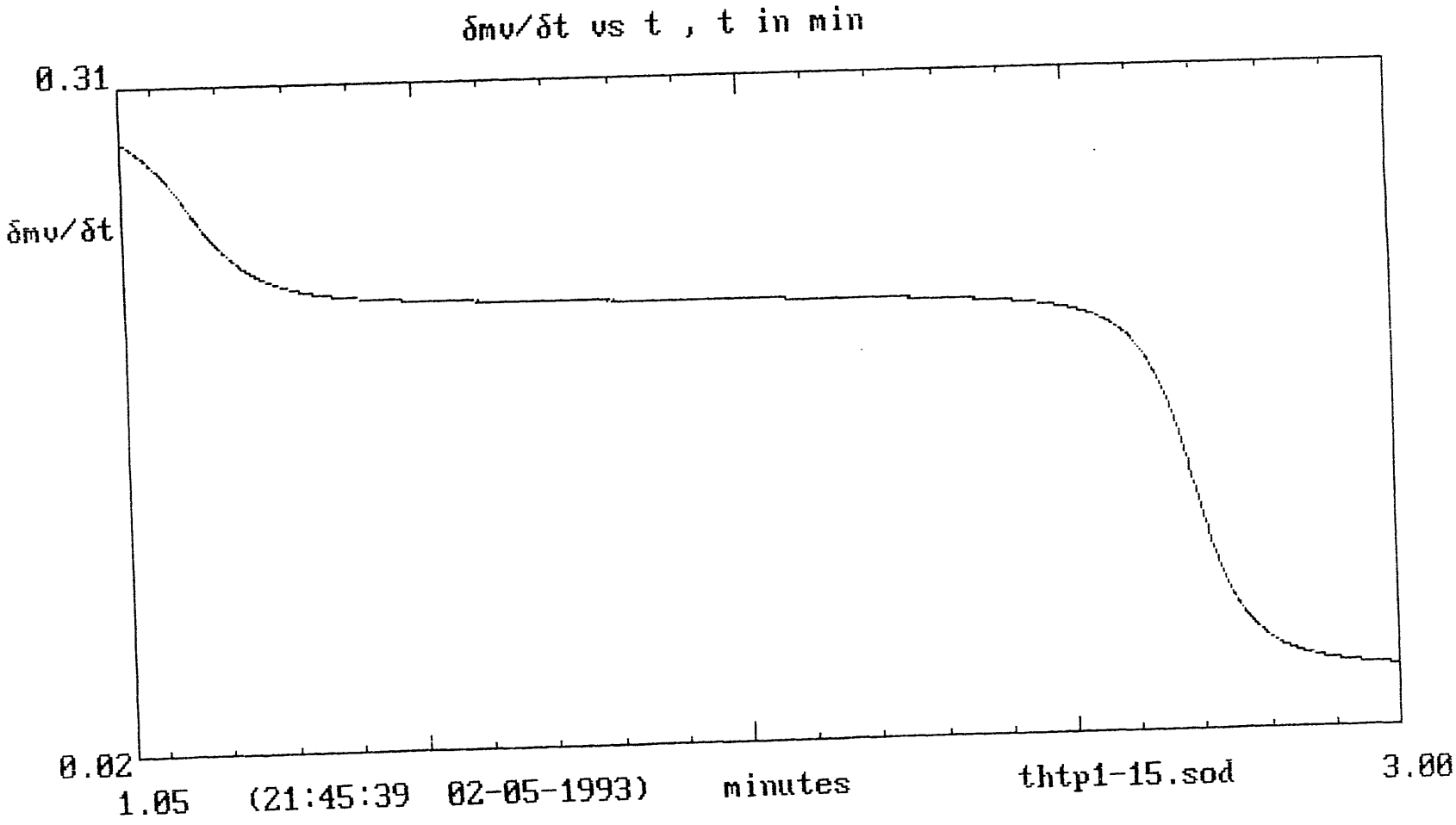

Figure 6d

Theoretical Model – Expanded Scale

$$\frac{\delta^2(mv)}{\delta t^2}$$

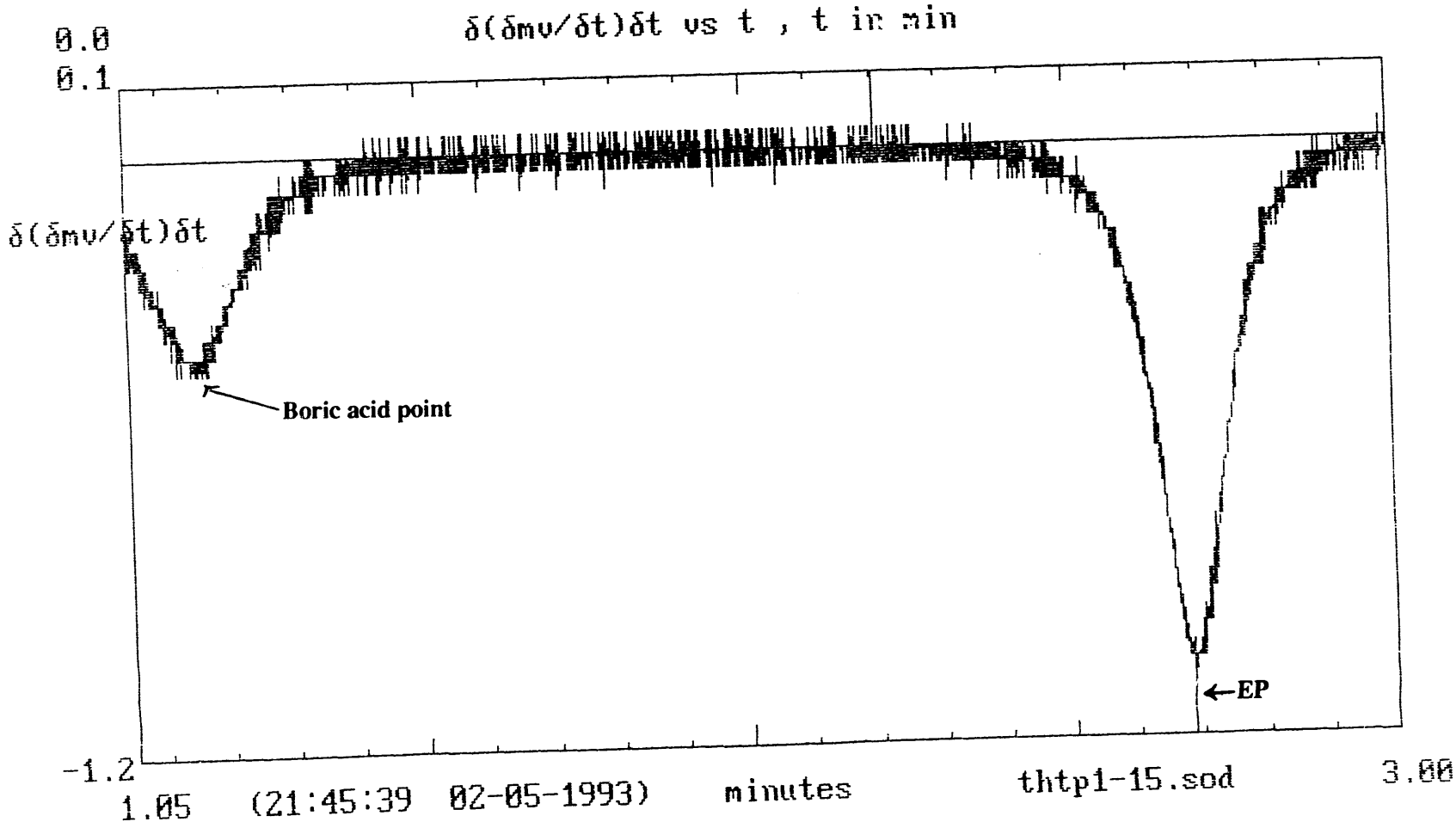

Figure 7a

Theoretical Thermogram With Noise (s.d. = 1 x 10^{-3} mv)

$$\frac{\delta(mv)}{\delta t}$$

No Smoothing

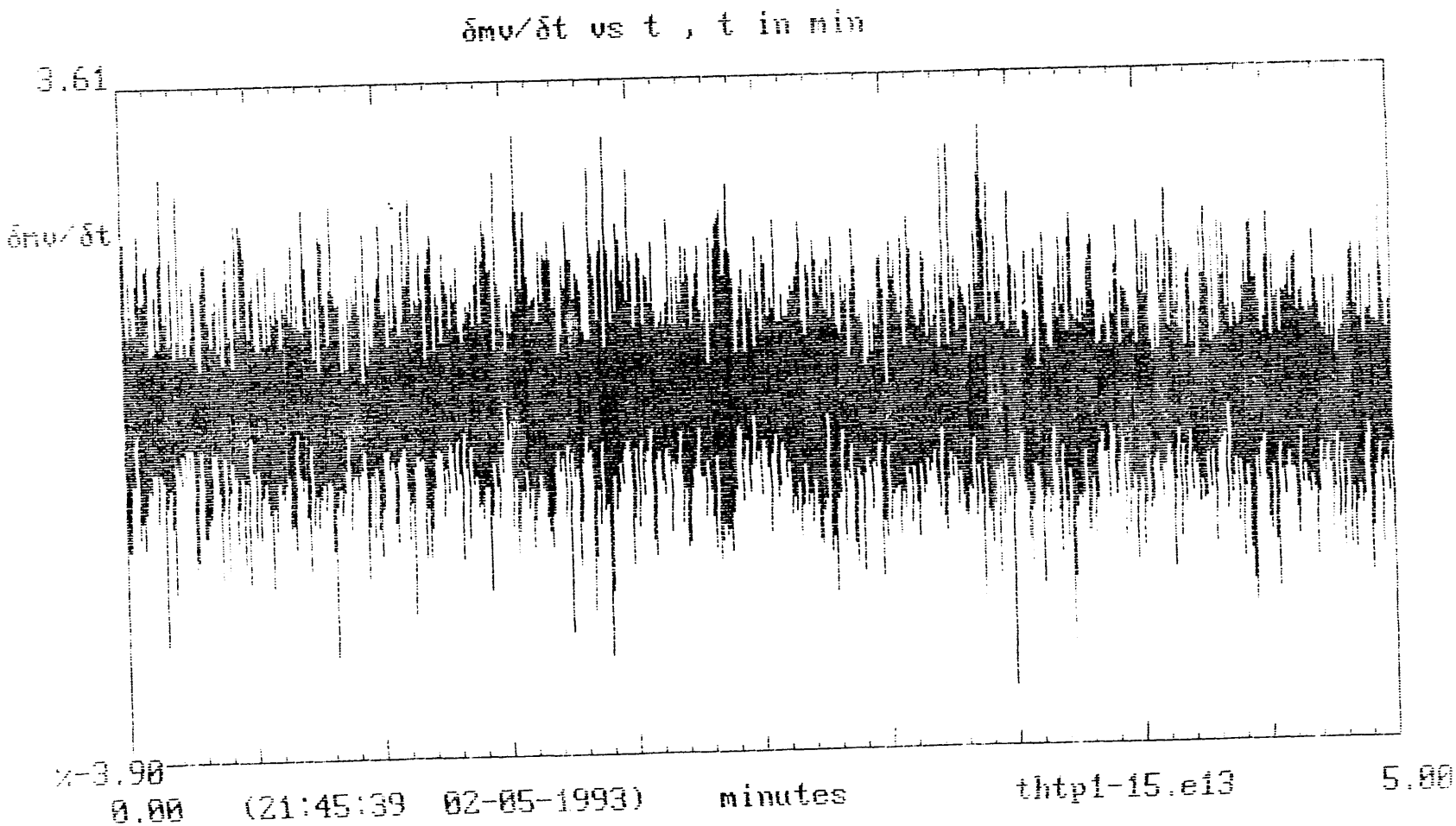

Figure 7b
Theoretical Thermogram With Noise (s.d. = 1 x 10^{-3} mv)

$$\frac{\delta^2(mv)}{\delta t^2}$$

No Smoothing

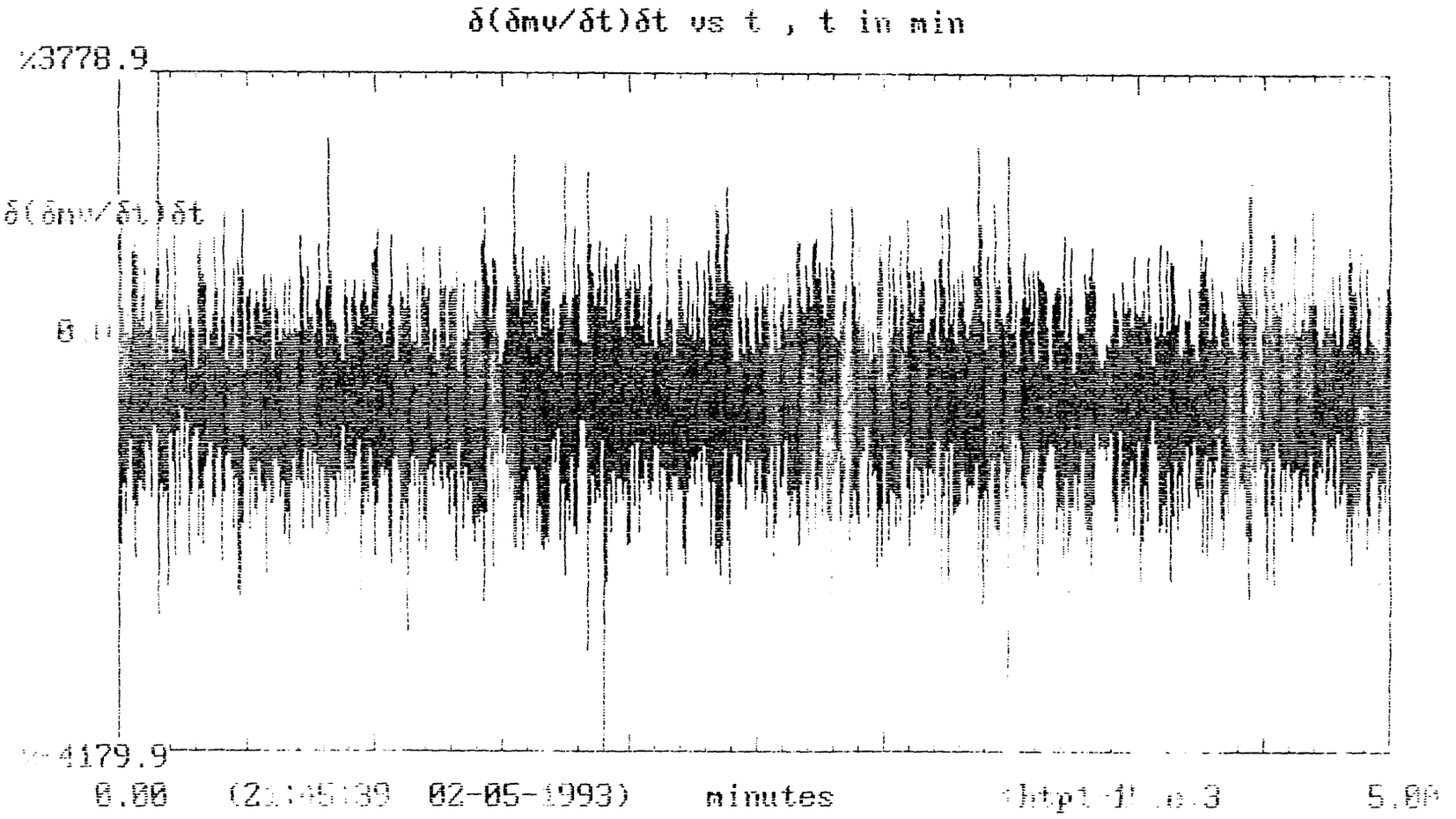

Figure 7c

Theoretical Model With Noise (s.d. = 1 x 10^{-3} mv)
Smoothing (~ 10pts)

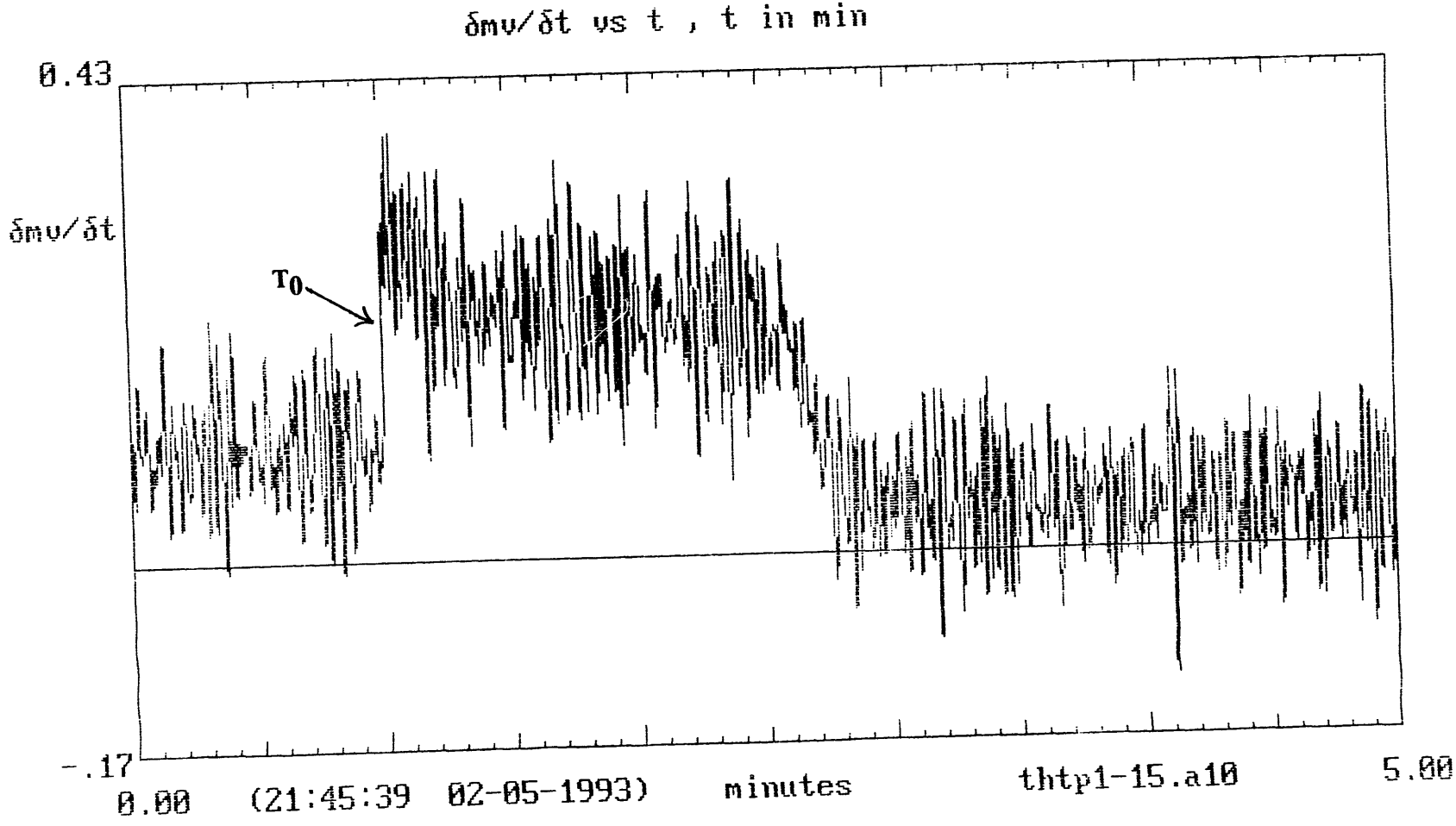

Figure 7d

Theoretical Model With Noise (s.d. = 1 x 10^{-3} mv)
Smoothing (~ 10pts)

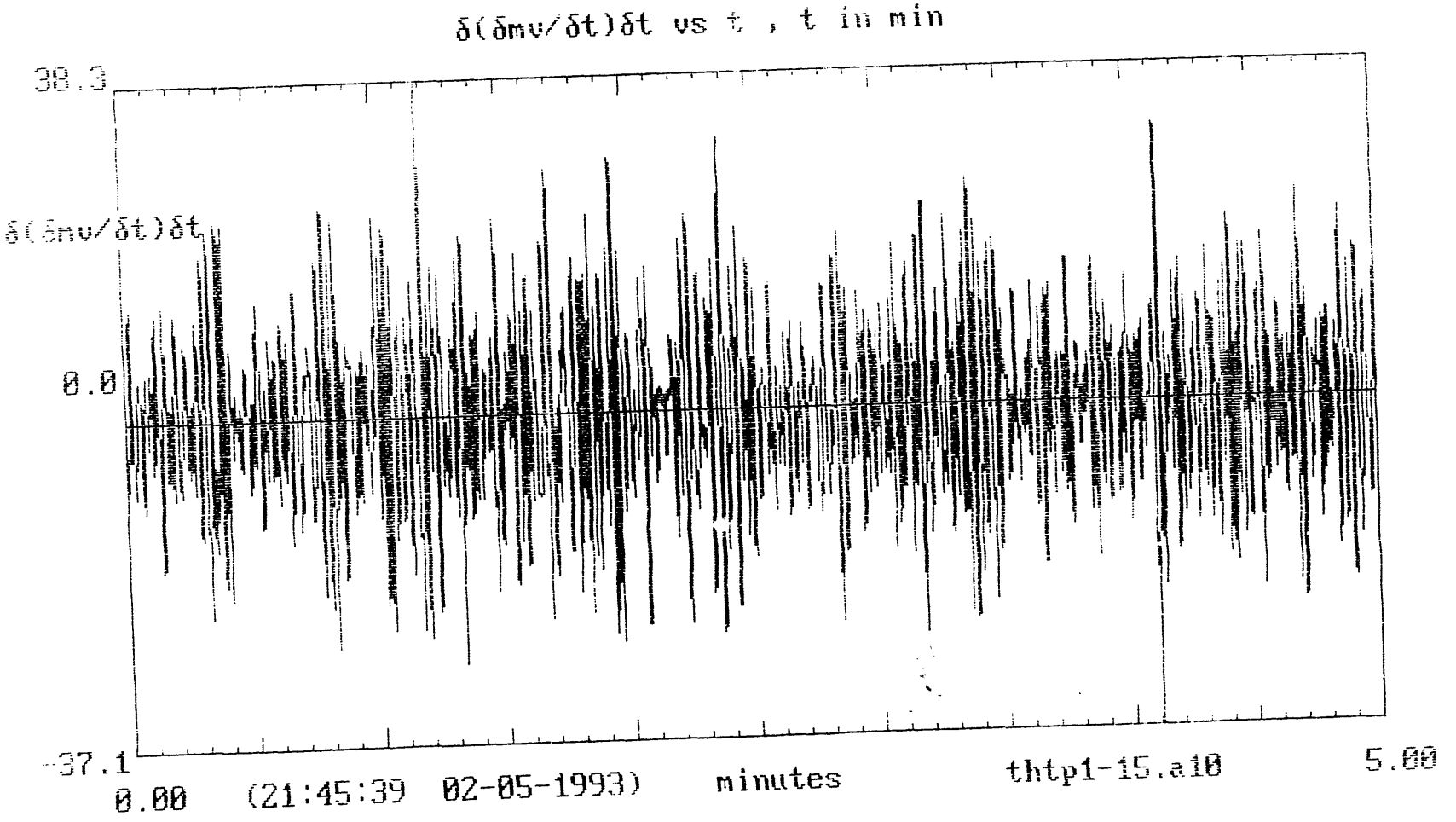

Figure 7e

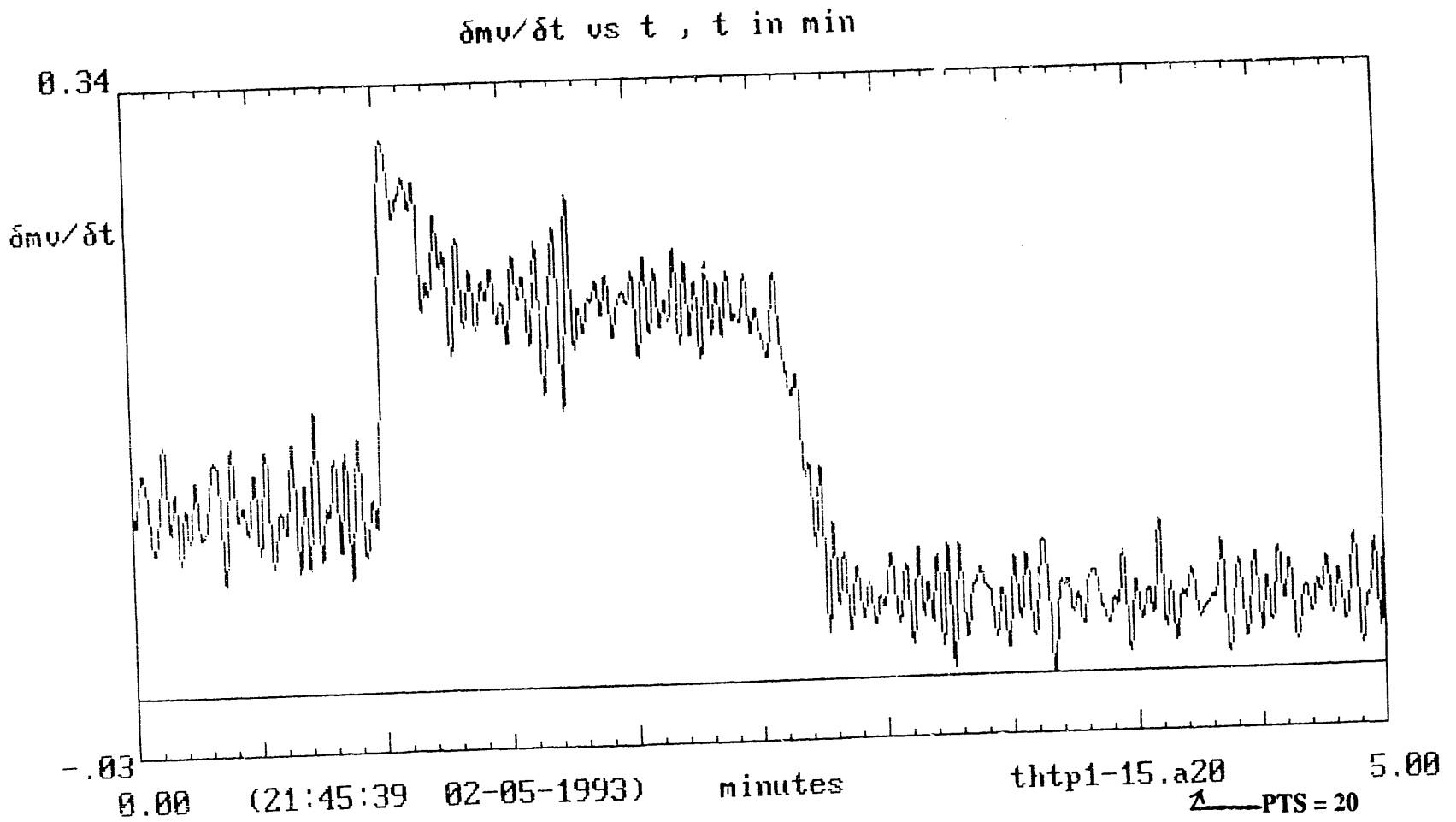
δmυ/δt vs t , t in min
0.34
δmυ/δt
-.03
0.00
(21:45:39 02-05-1993)
minutes
thtp1-15.a20
5.00
PTS = 20

Figure 7f

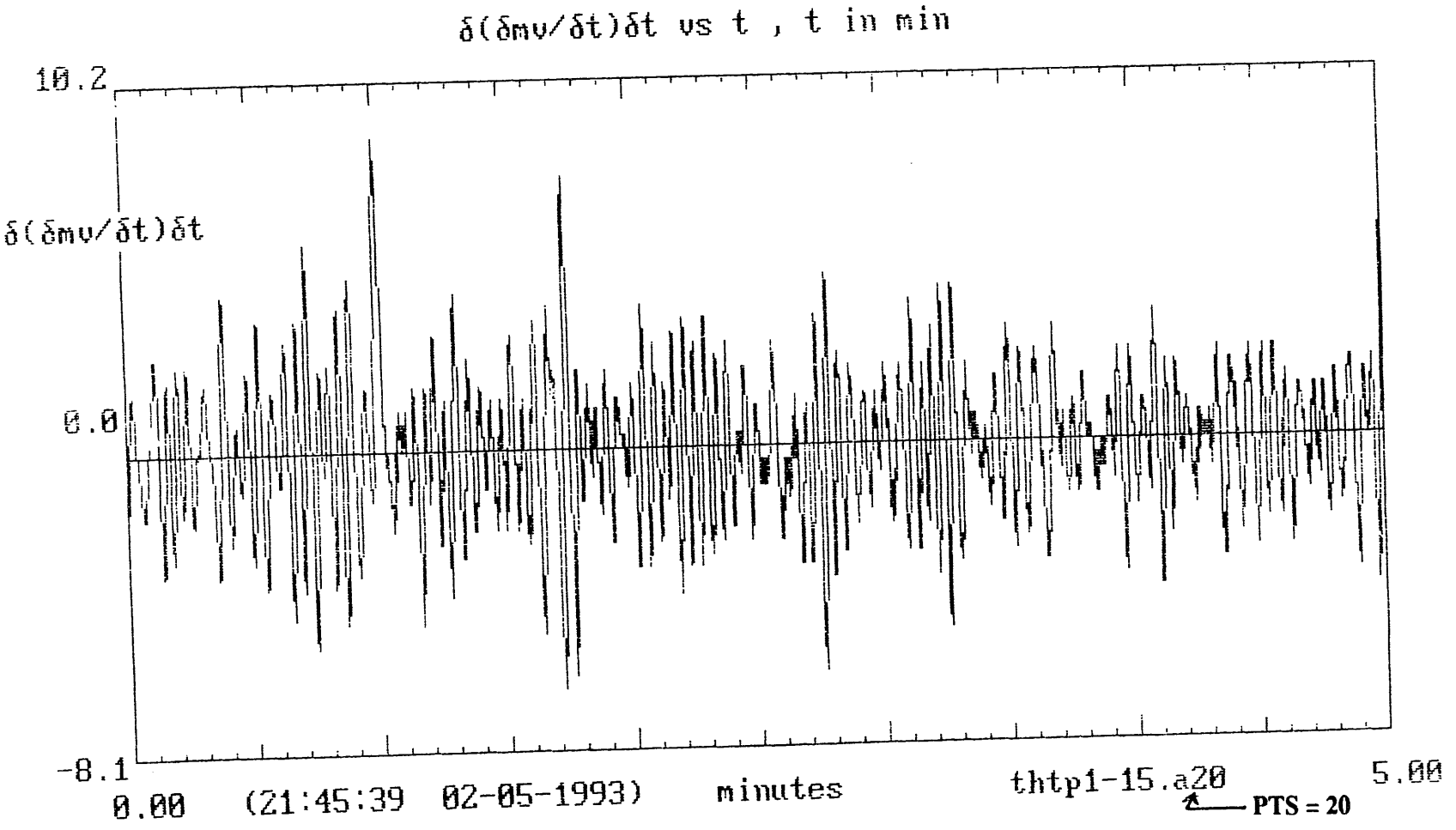
δ(δmv/δt)δt vs t , t in min
10.2
δ(δmv/δt)δt
0.0
-8.1
0.00
(21:45:39 02-05-1993)
minutes
thtp1-15.a20
5.00
PTS = 20

Figure 7g

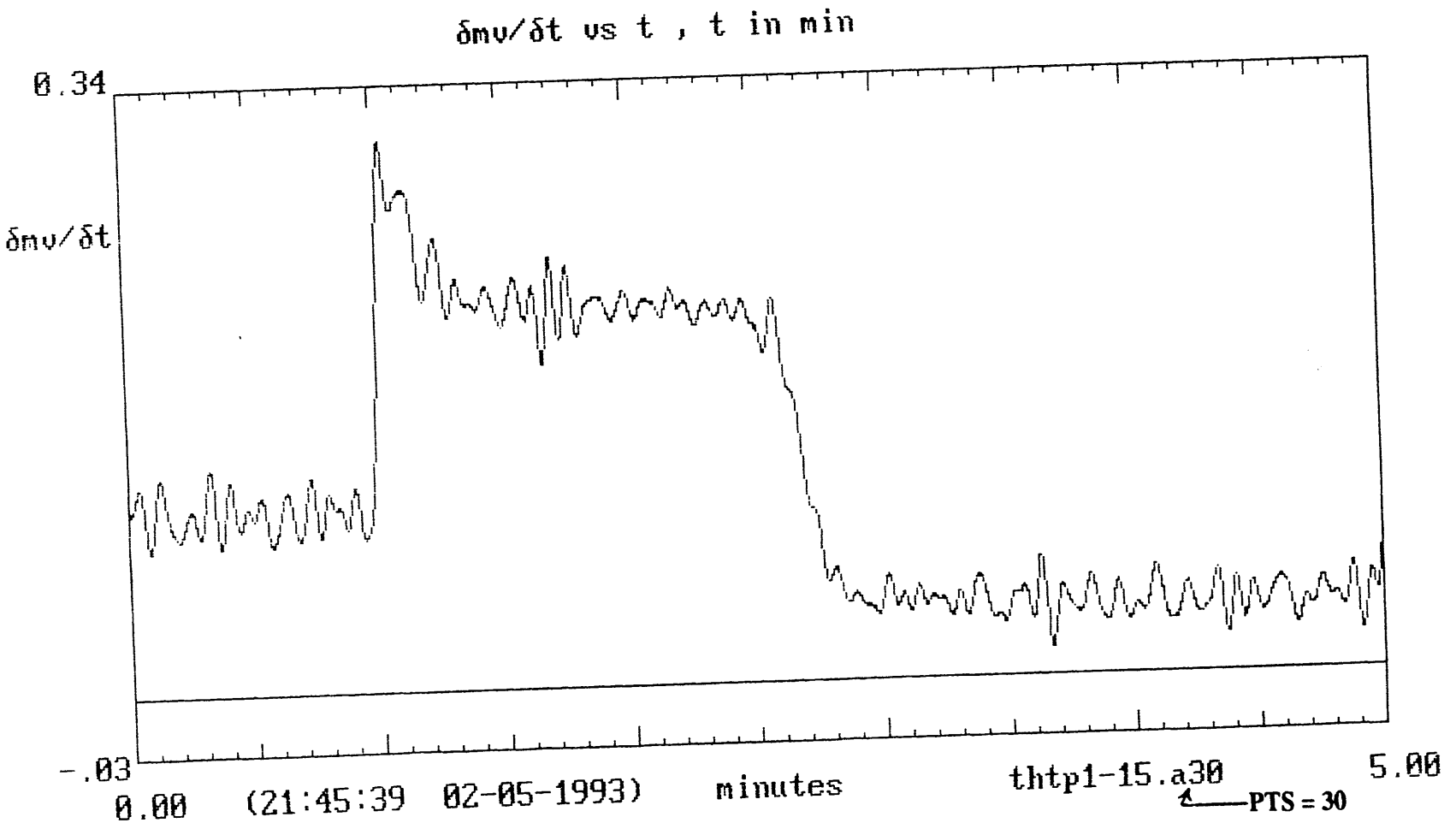
δmυ/δt vs t , t in min
0.34
δmυ/δt
-.03
0.00
(21:45:39 02-05-1993)
minutes
thtp1-15.a30
5.00
PTS = 30

Figure 7h

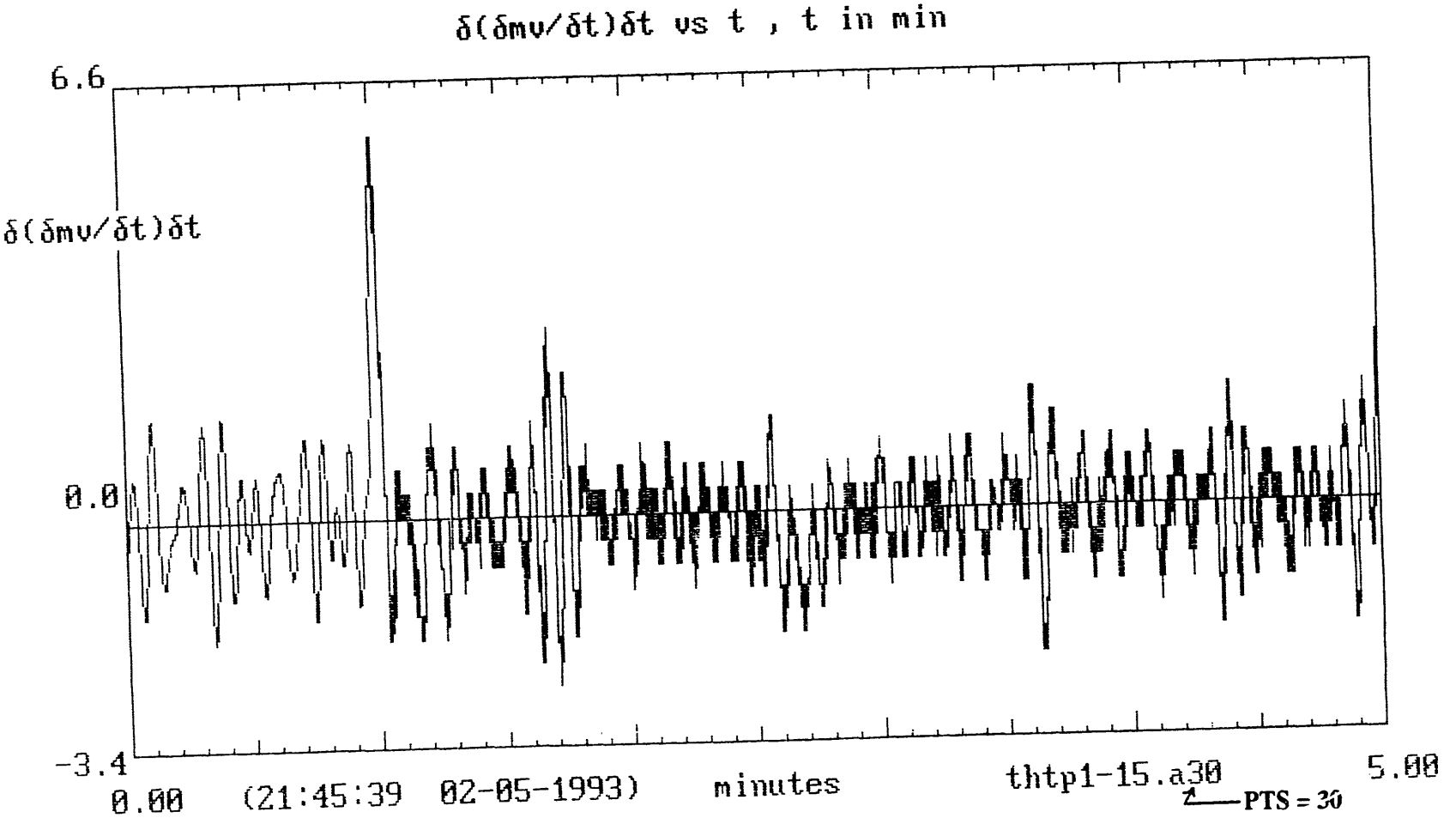
δ(δmv/δt)δt vs t , t in min
6.6
δ(δmv/δt)δt
0.0
-3.4
0.00
(21:45:39 02-05-1993)
minutes
thtp1-15.a30
5.00
PTS = 30

Figure 7i

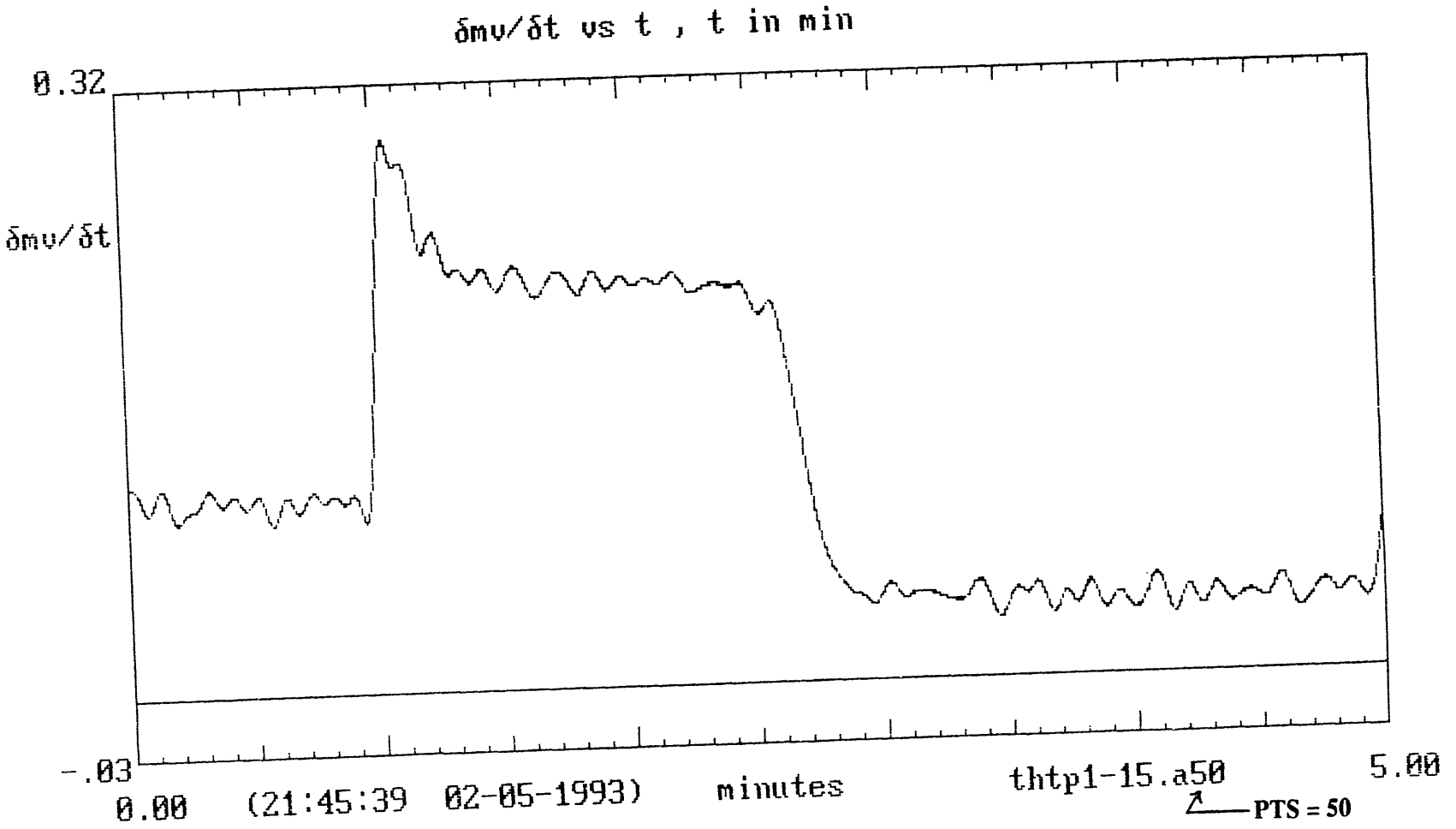
δmv/δt vs t , t in min
0.32
δmv/δt
-.03
0.00
(21:45:39 02-05-1993)
minutes
thtp1-15.a50
5.00
PTS = 50

Figure 7j

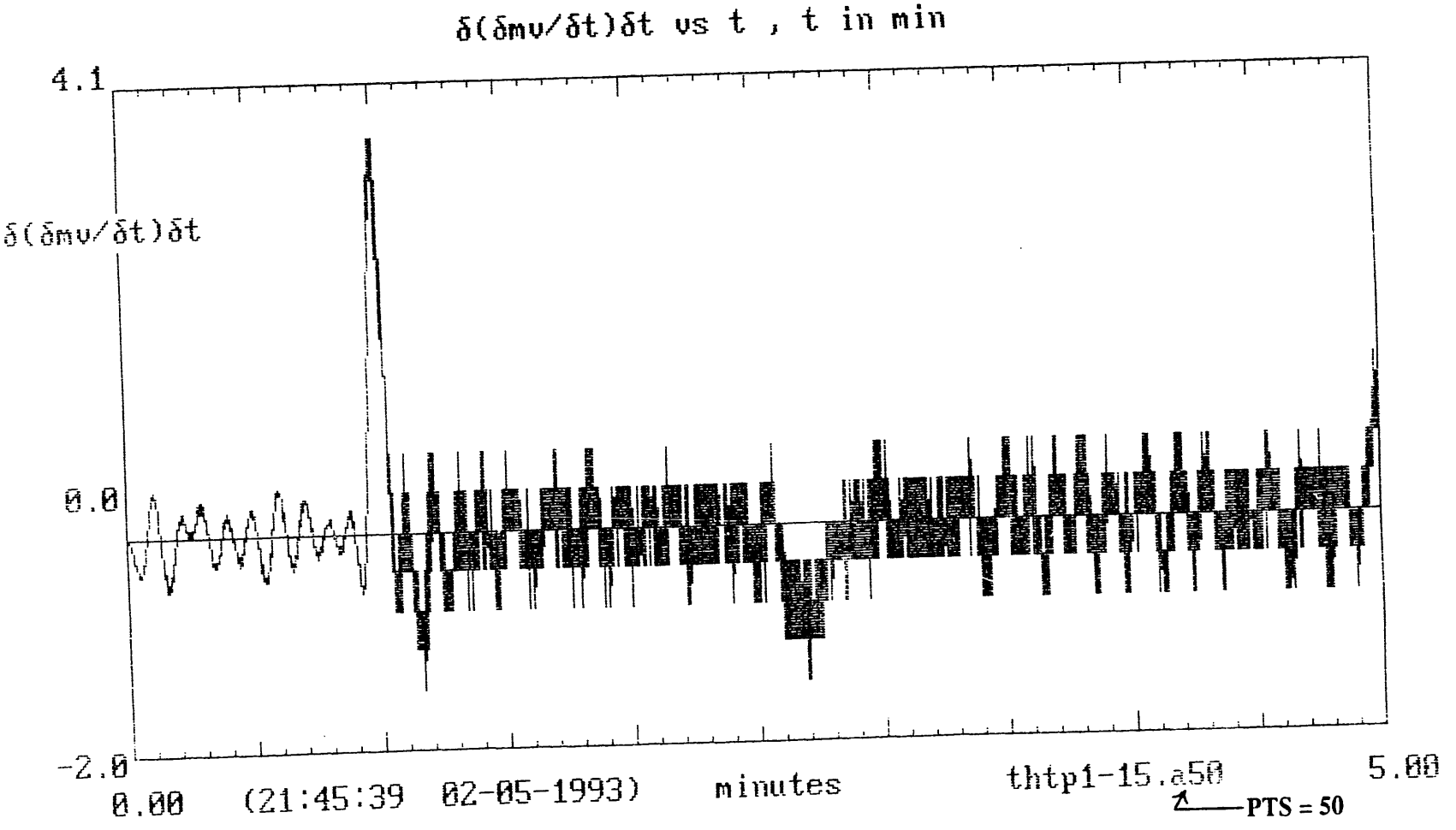
δ(δmv/δt)δt vs t , t in min
4.1
δ(δmv/δt)δt
0.0
-2.0
0.00
(21:45:39 02-05-1993)
minutes
thtp1-15.a50
5.00
PTS = 50

Figure 7k

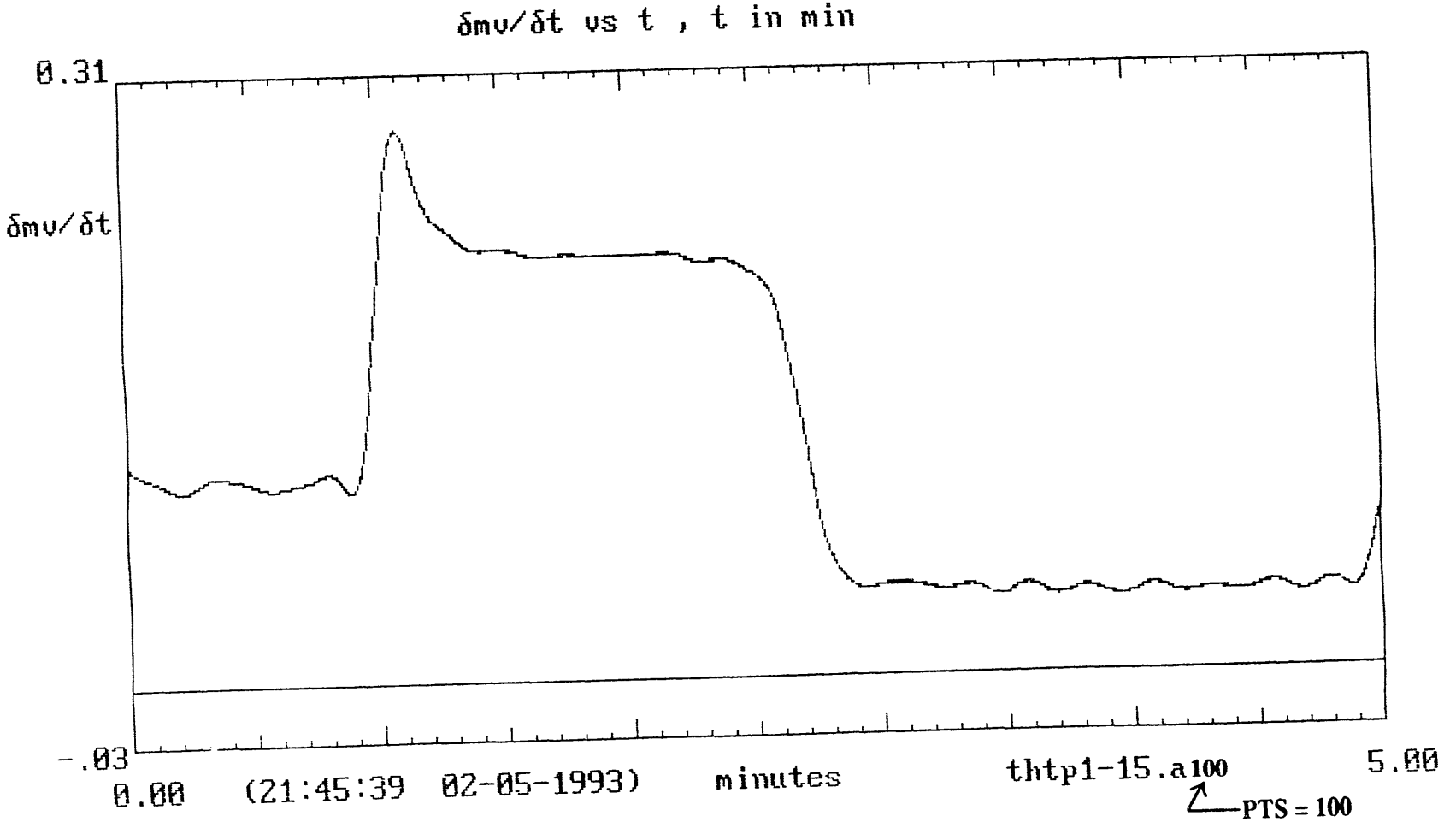
δmυ/δt vs t , t in min
0.31
δmυ/δt
-.03
0.00
(21:45:39 02-05-1993)
minutes
thtp1-15.a100
5.00
PTS = 100

Figure 7l

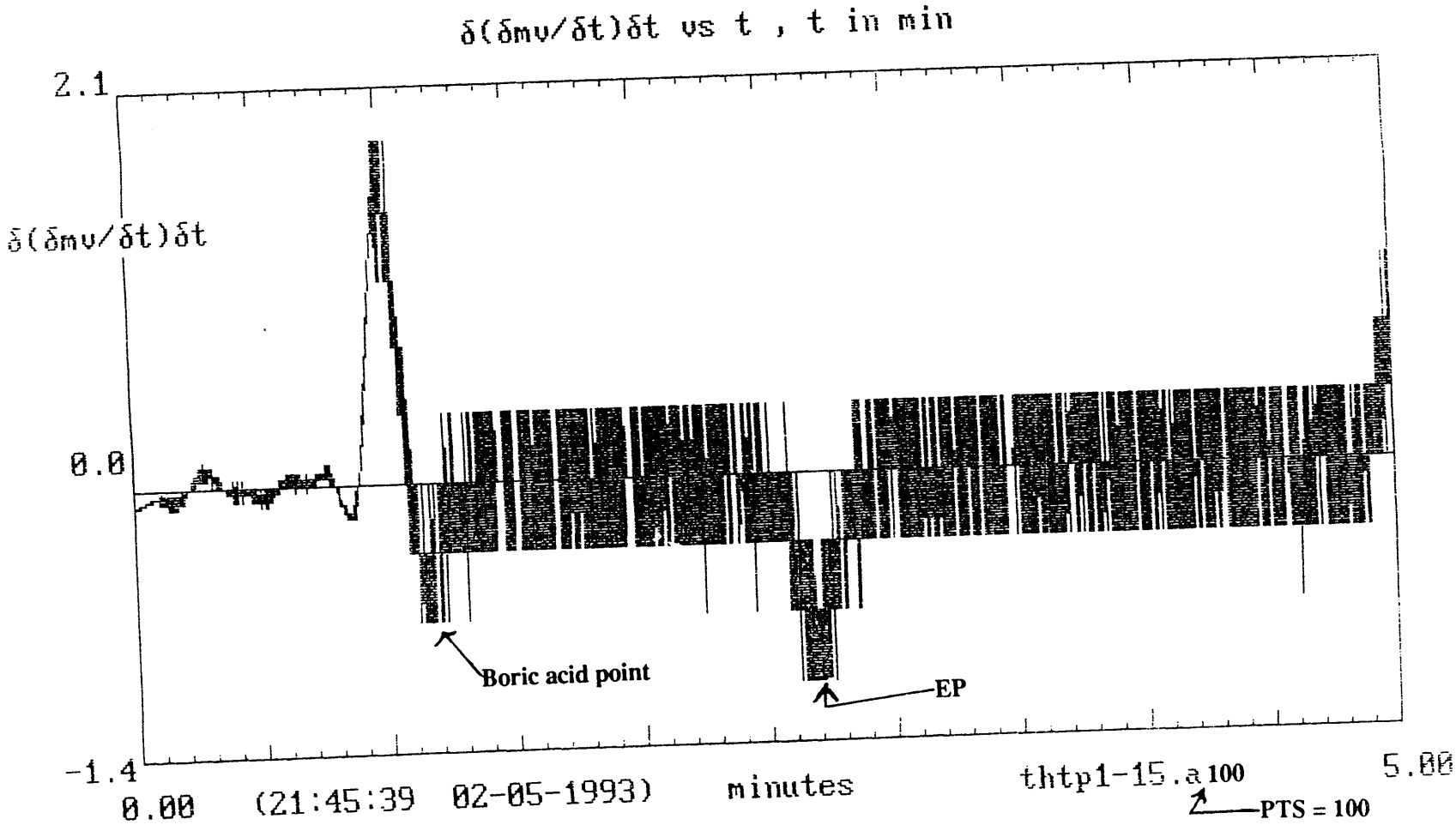
δ(δmv/δt)δt vs t , t in min
2.1
δ(δmv/δt)δt
0.0
-1.4
Boric acid point
EP
0.00
(21:45:39 02-05-1993)
minutes
thtp1-15.a100
5.00
PTS = 100

Figure 8a

$$\frac{\delta(mv)}{\delta t}$$

Sample NS11

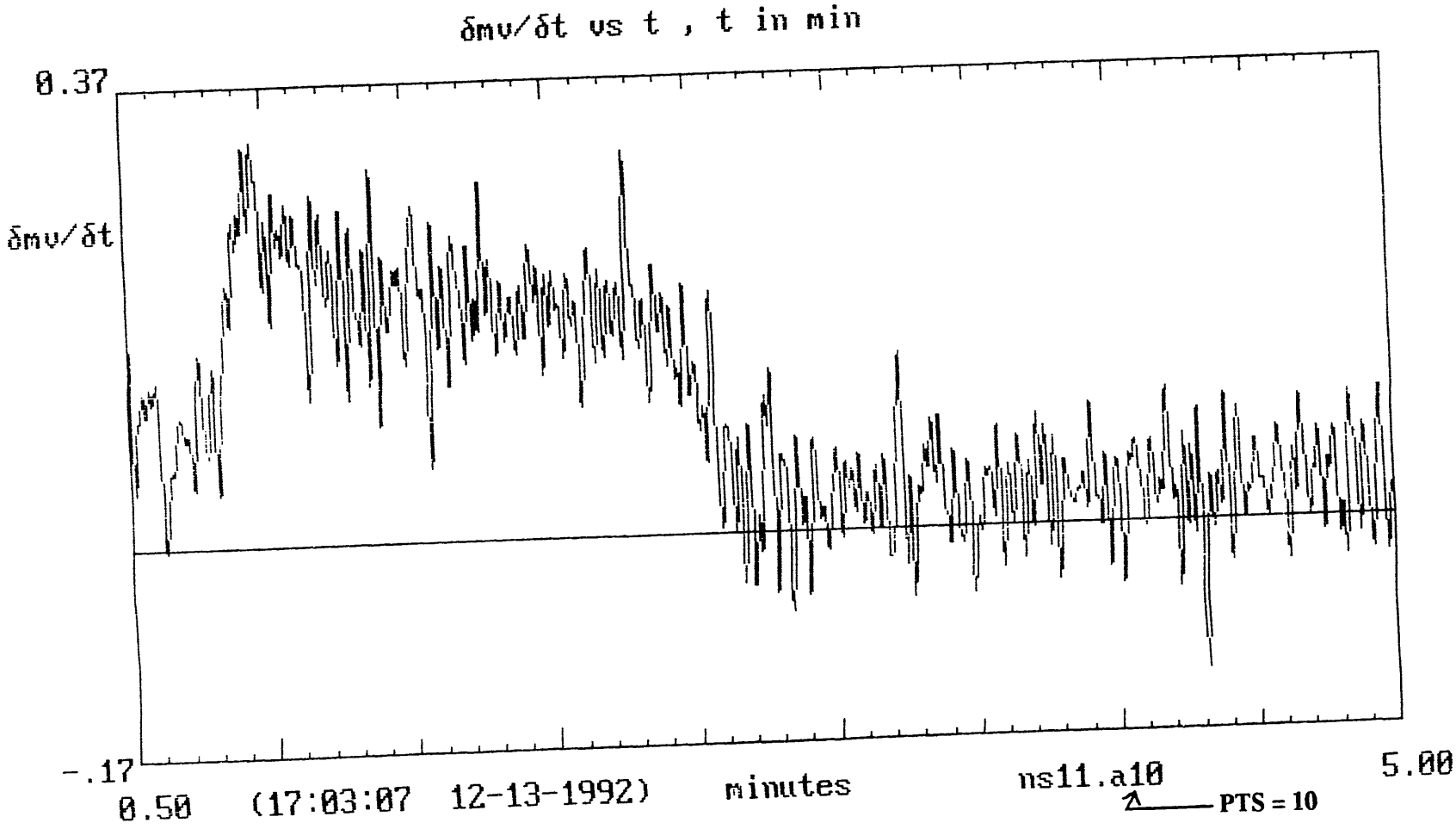

Figure 8b

$$\frac{\delta^2(mv)}{\delta t^2}$$

Sample NS11

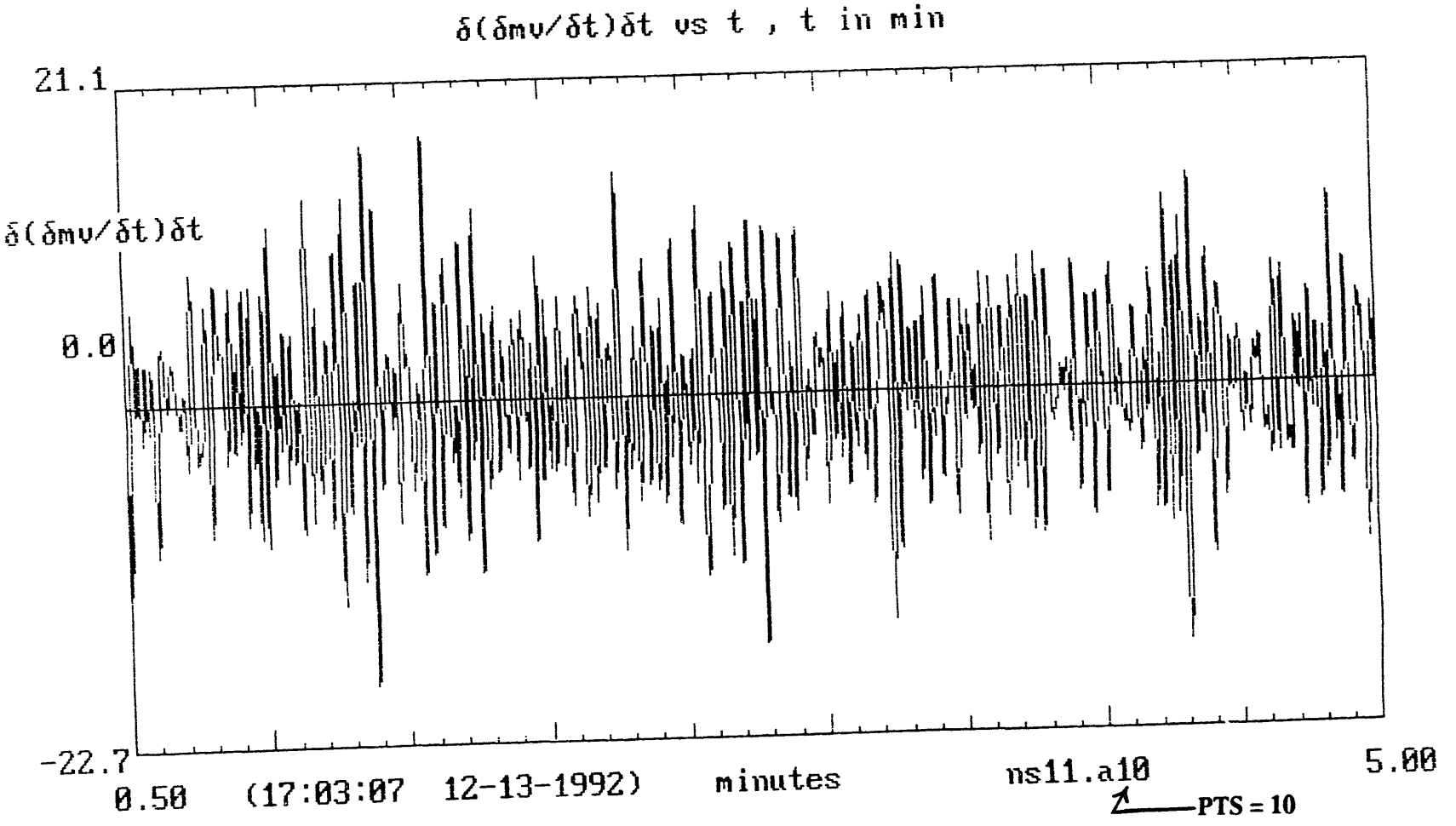

Figure 8c

$$\frac{\delta(mv)}{\delta t}$$

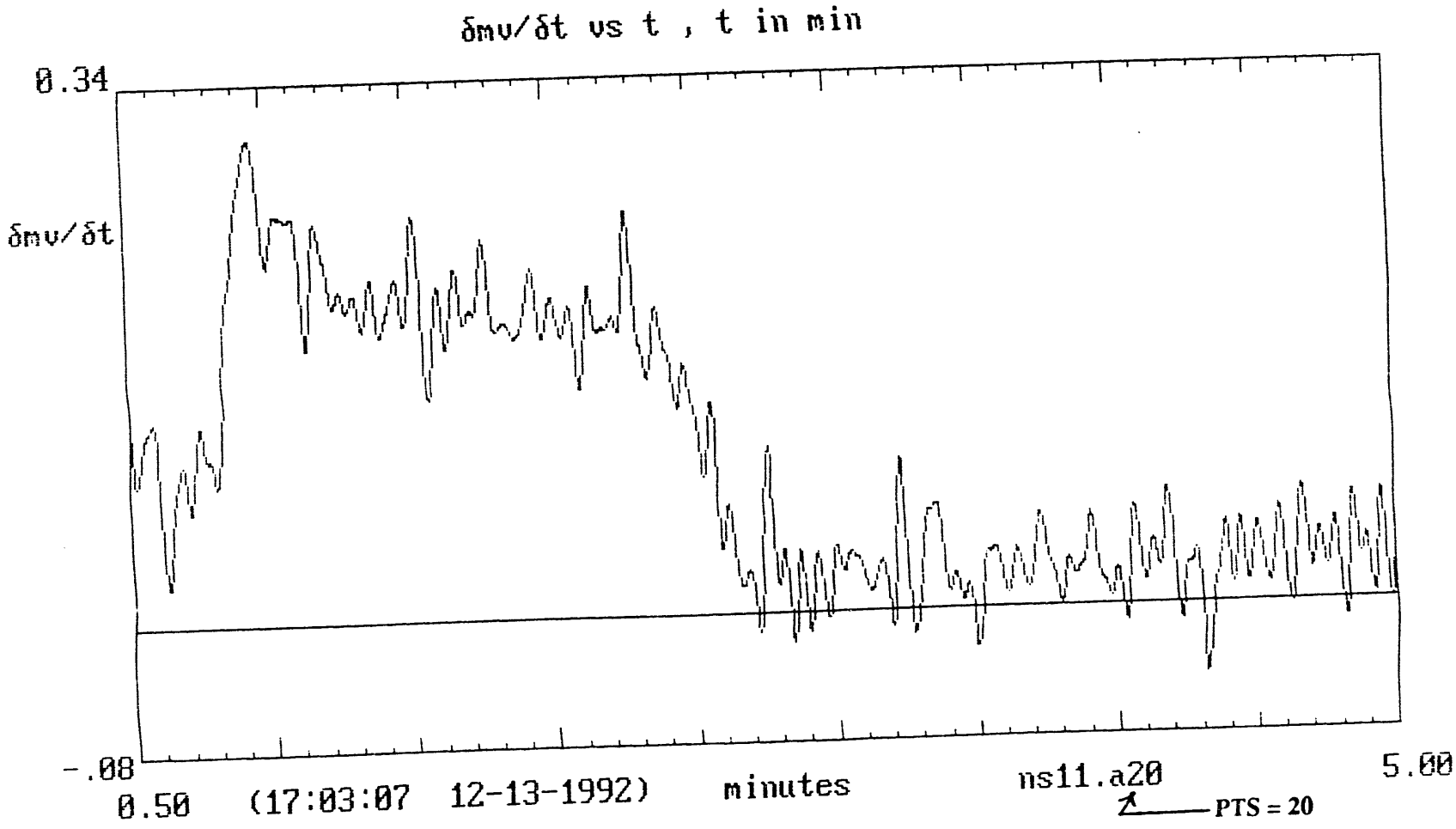

Figure 8d

$$\frac{\delta^2(mv)}{\delta t^2}$$

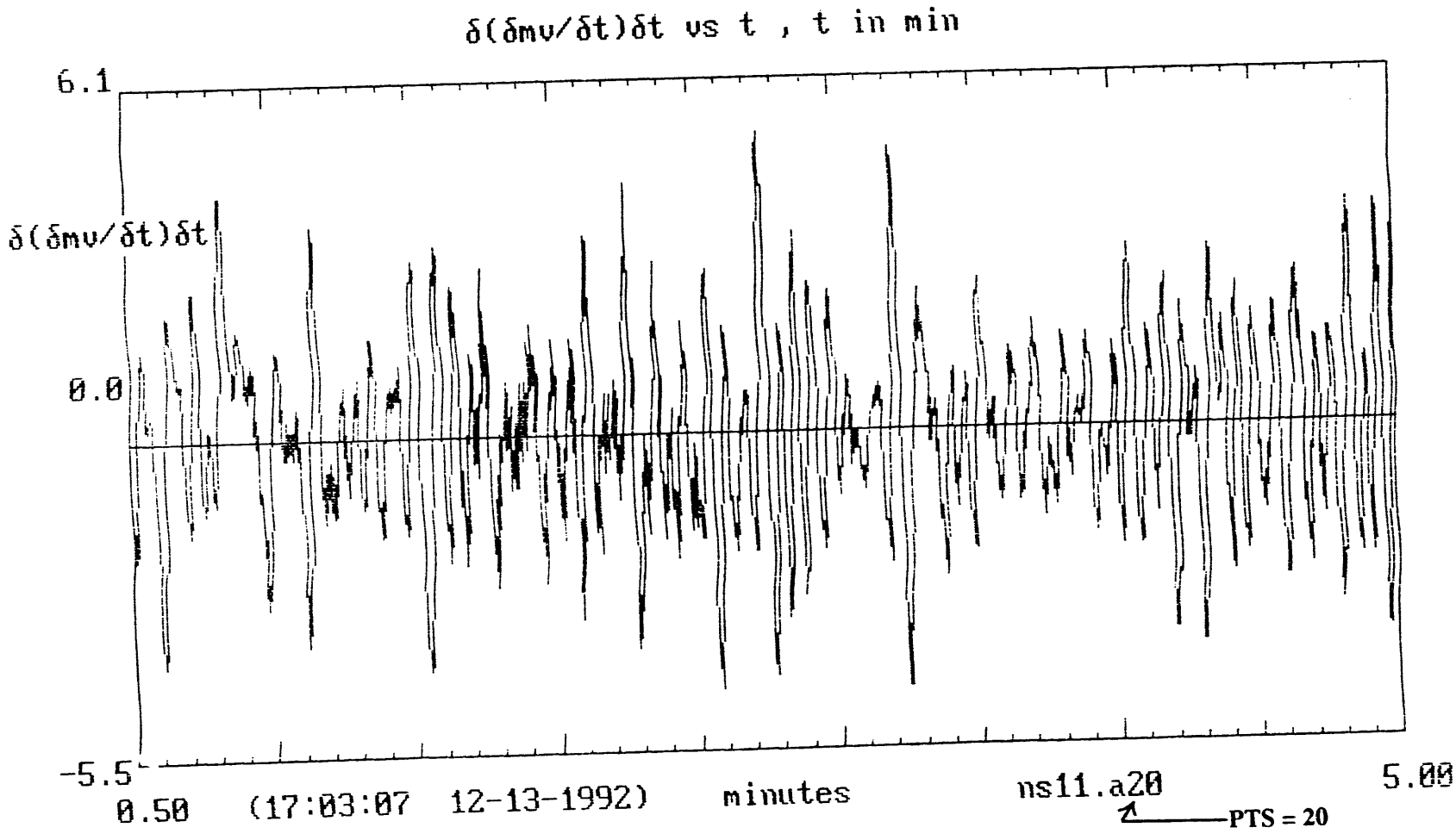

Figure 9a

Thermogram for Sample MILLSW3
Acid Pre-Addition Method

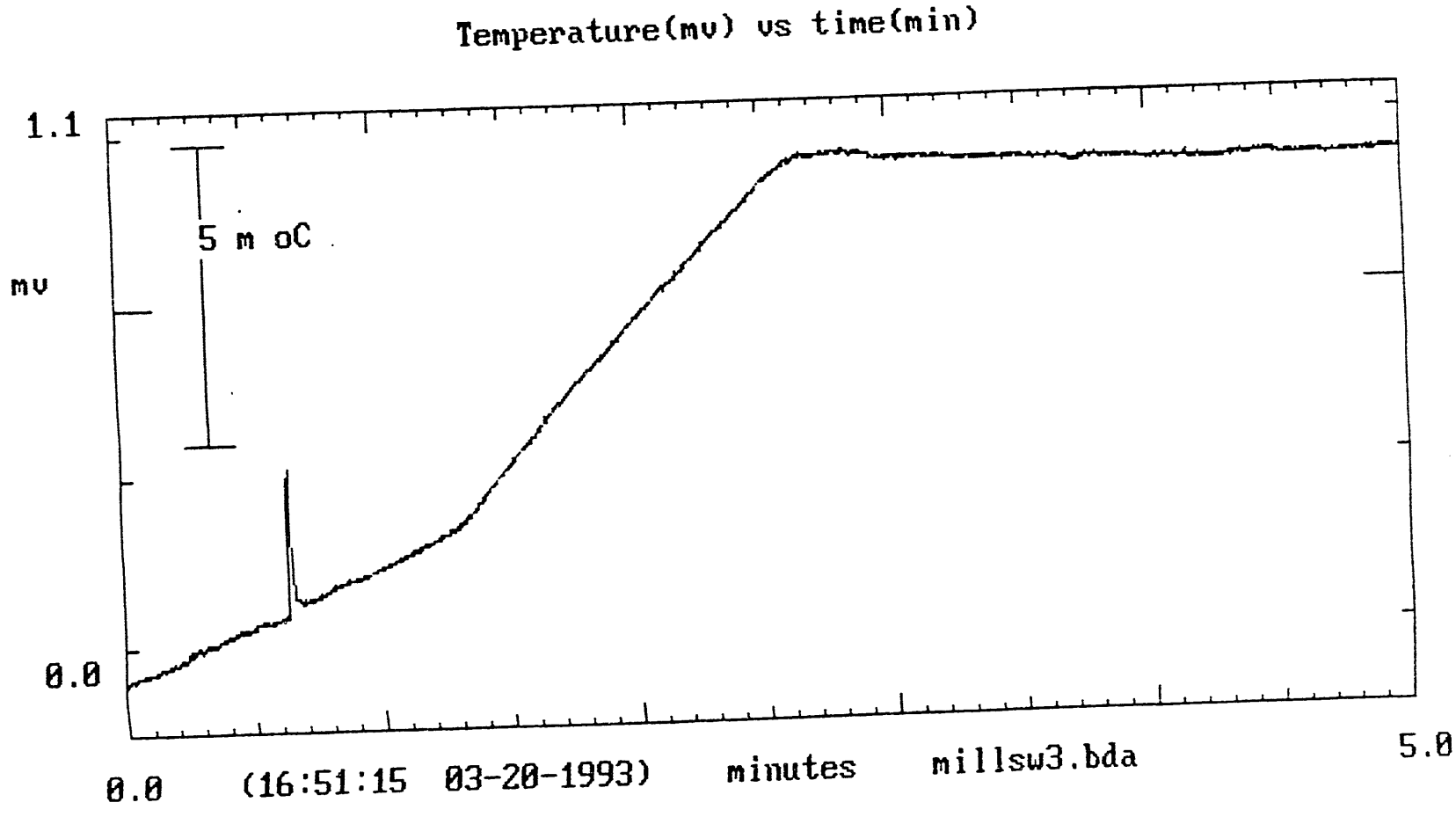

Figure 9b

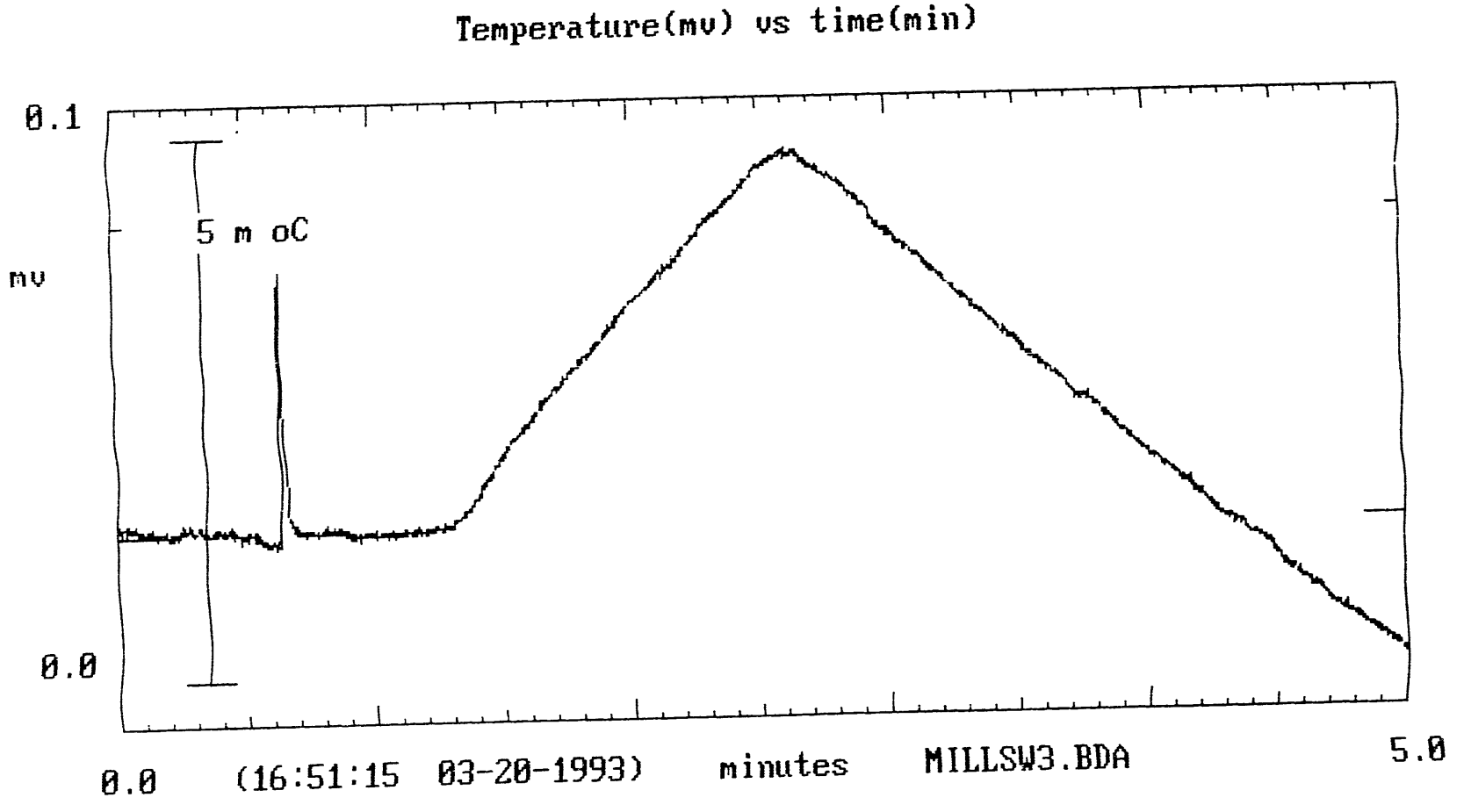
Temperature(mv) vs time(min)
0.1
5 m oC
mv
0.0
0.0
(16:51:15 03-20-1993)
minutes
MILLSW3.BDA
5.0

Figure 9c

Thermogram for MILLSW3

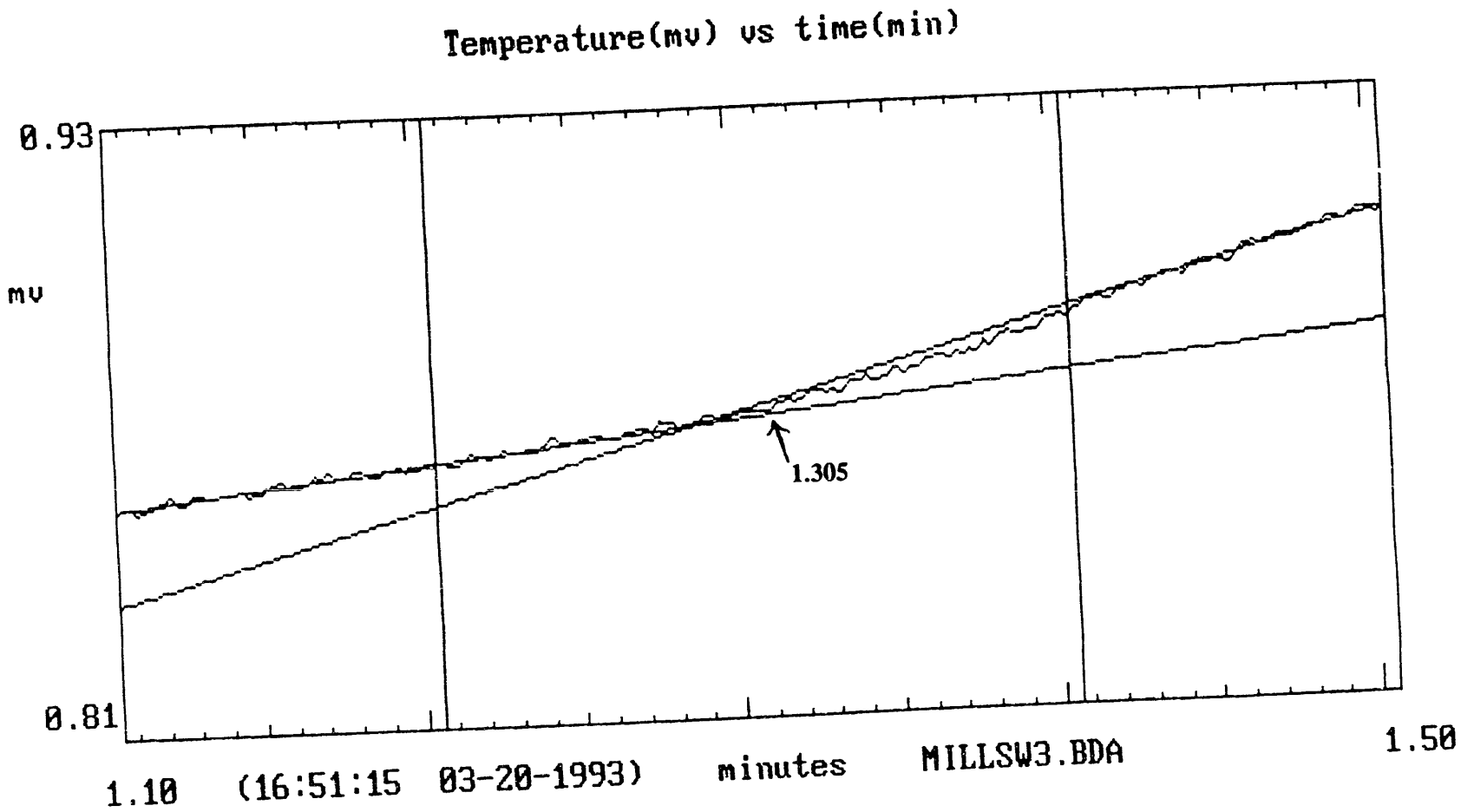

Figure 9d

Thermogram for MILLSW3

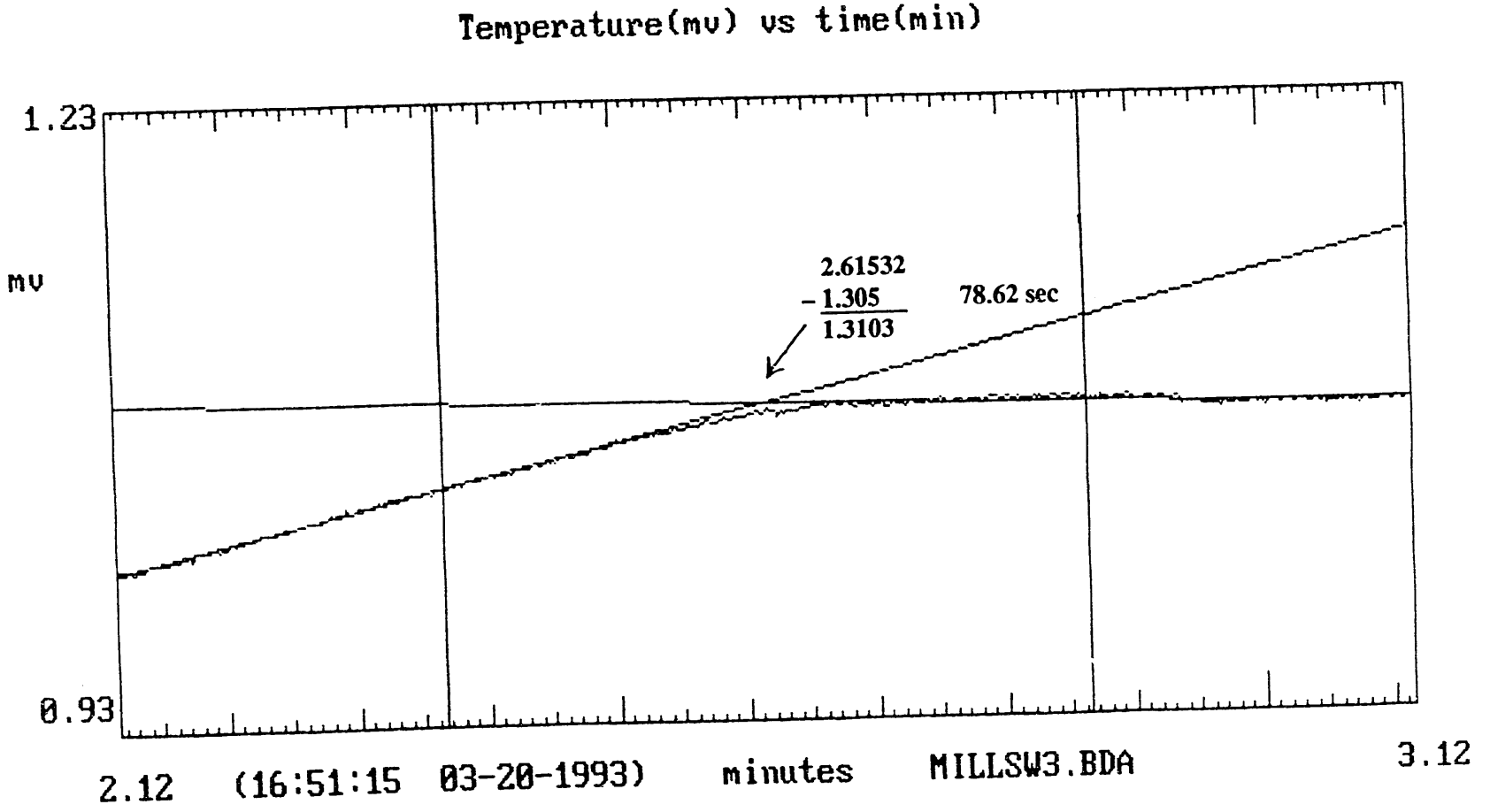

Figure 10a

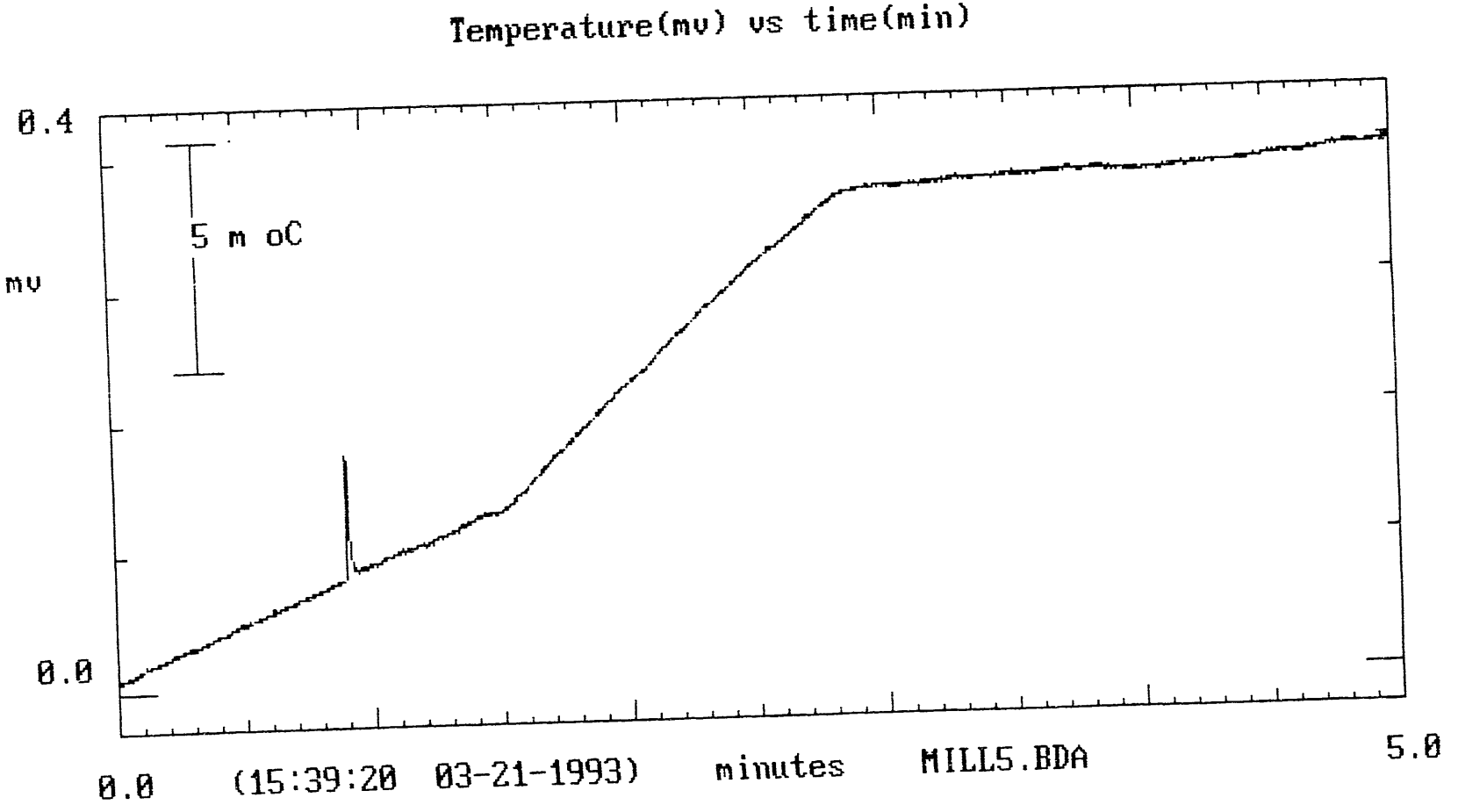
Temperature(mv) vs time(min)
0.4
5 m oC
mv
0.0
0.0
(15:39:20 03-21-1993)
minutes
MILL5.BDA
5.0

Figure 10b

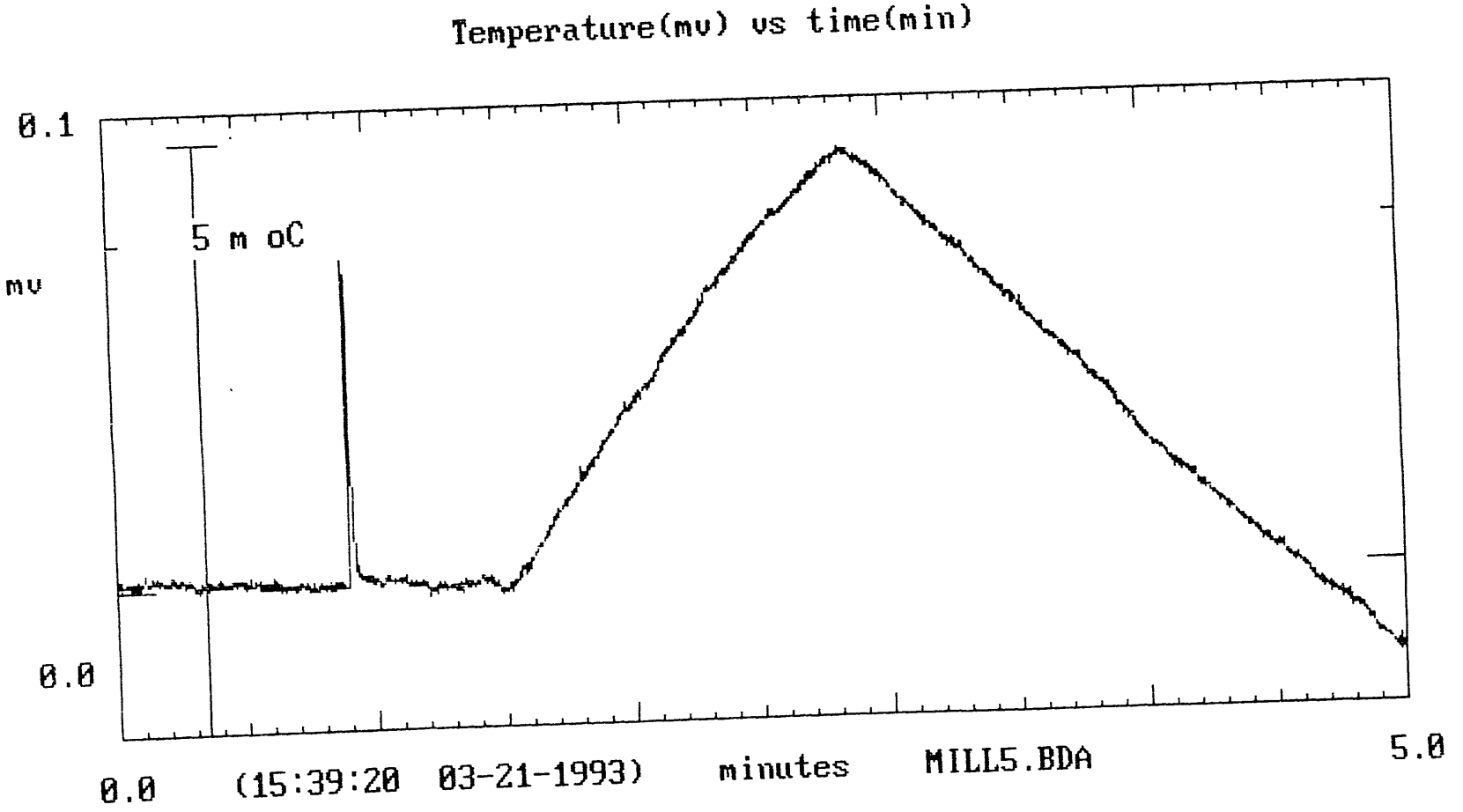
Temperature(mv) vs time(min)
0.1
5 m oC
mv
0.0
0.0
(15:39:20 03-21-1993)
minutes
MILL5.BDA
5.0

Figure 10c

2.7976 – 1.5544 = 1.2432 min
74.59 sec
74.59 + 29.45 = 104.04

RT = 1.2432 min
± 0.00376
0.30%

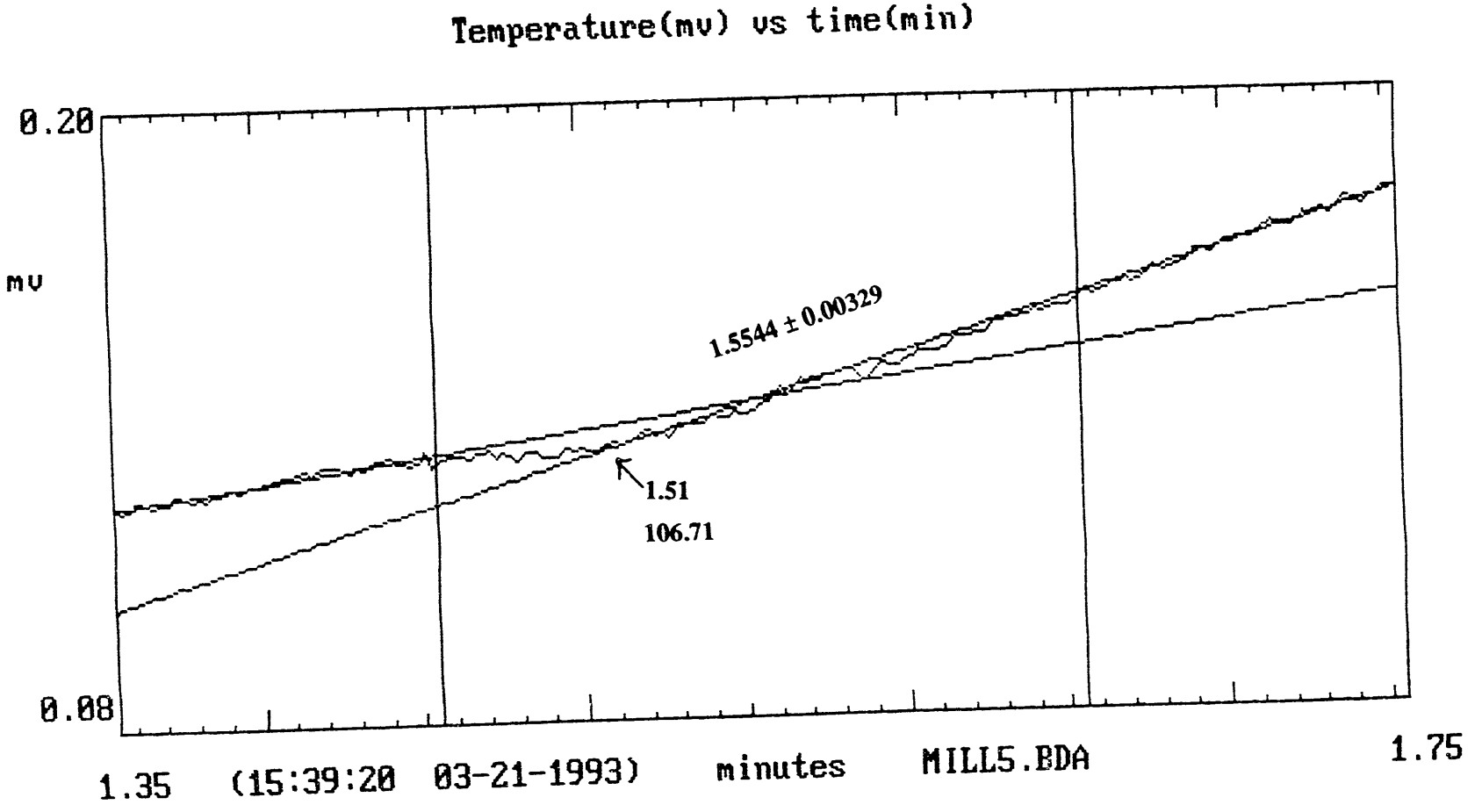

Figure 10c'

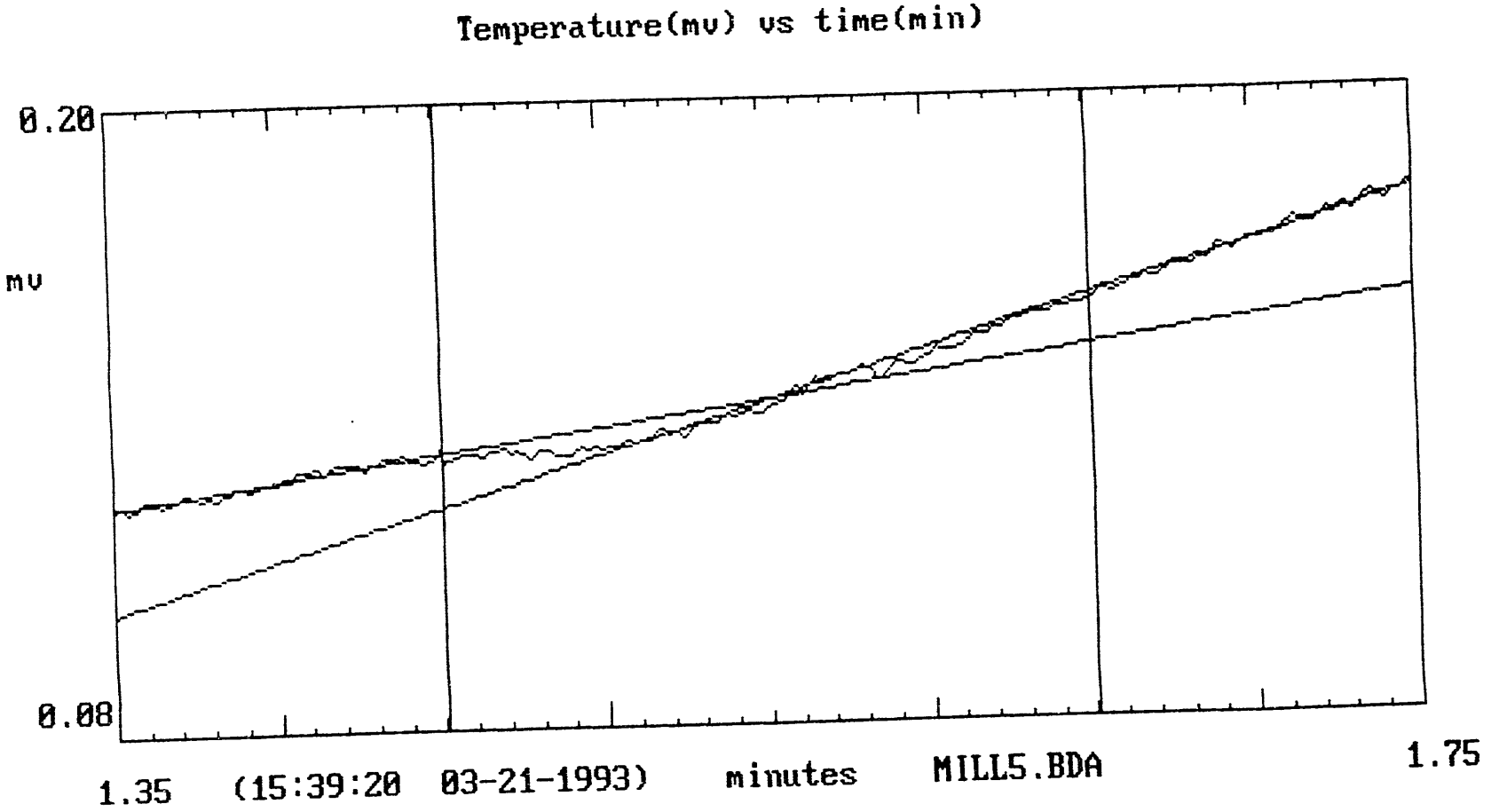
Temperature(mv) vs time(min)
0.20
mv
0.08
1.35
(15:39:20 03-21-1993)
minutes
MILL5.BDA
1.75

Figure 10d

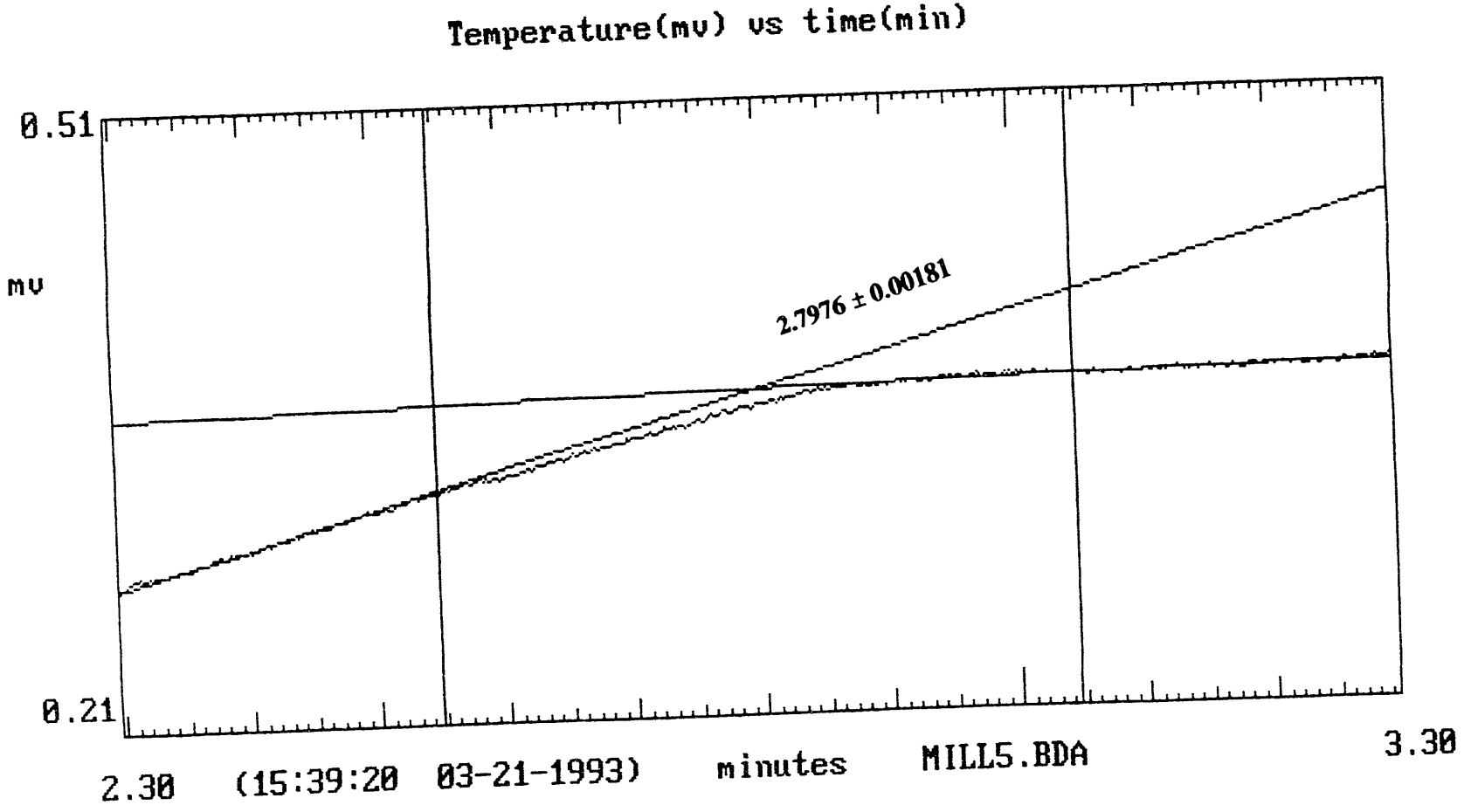
Temperature(mv) vs time(min)
0.51
mv
0.21
2.7976 ± 0.00181
2.30
(15:39:20 03-21-1993)
minutes
MILL5.BDA
3.30

Figure 11a

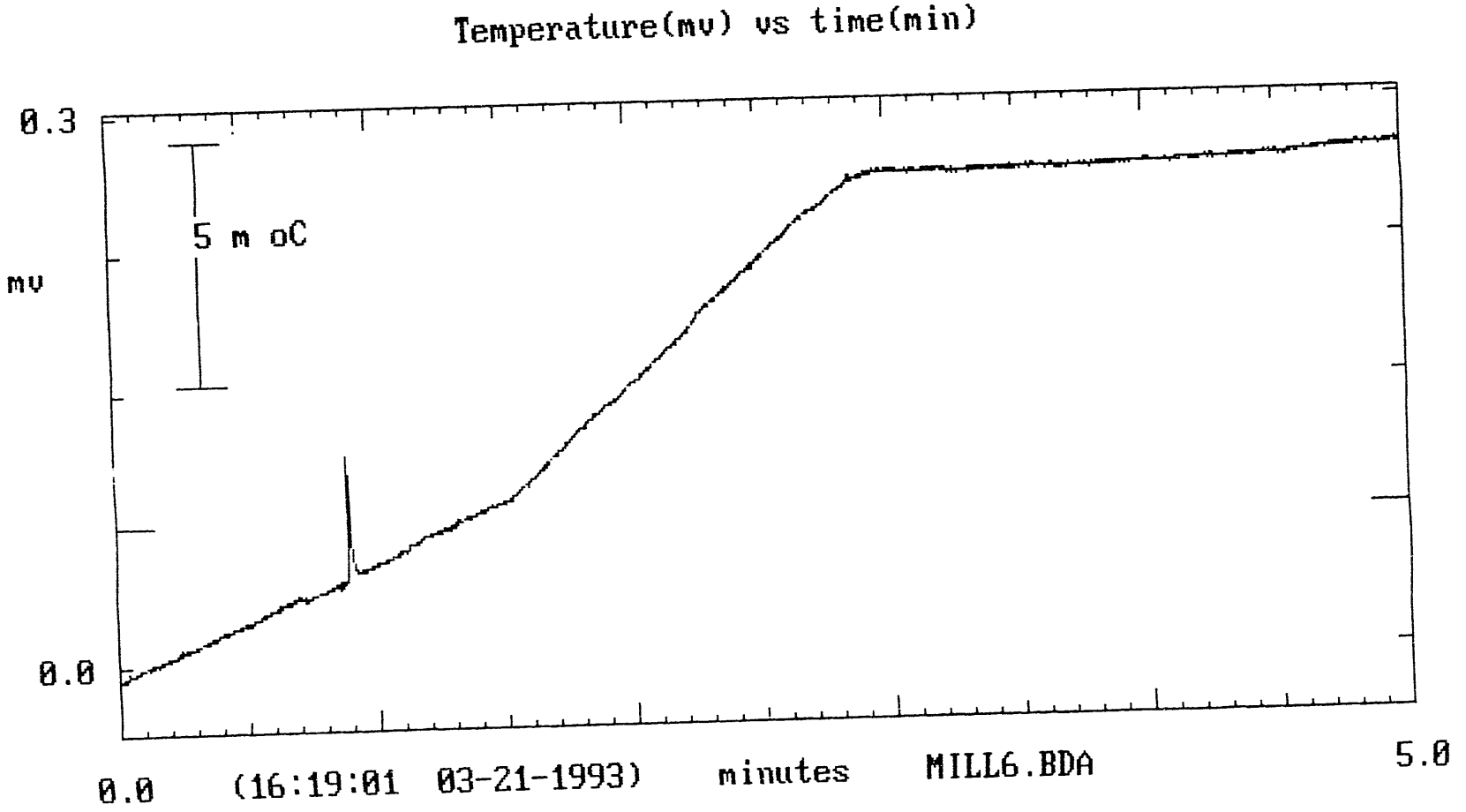
Temperature(mv) vs time(min)
0.3
5 m oC
mv
0.0
0.0
(16:19:01 03-21-1993)
minutes
MILL6.BDA
5.0

Figure 11b

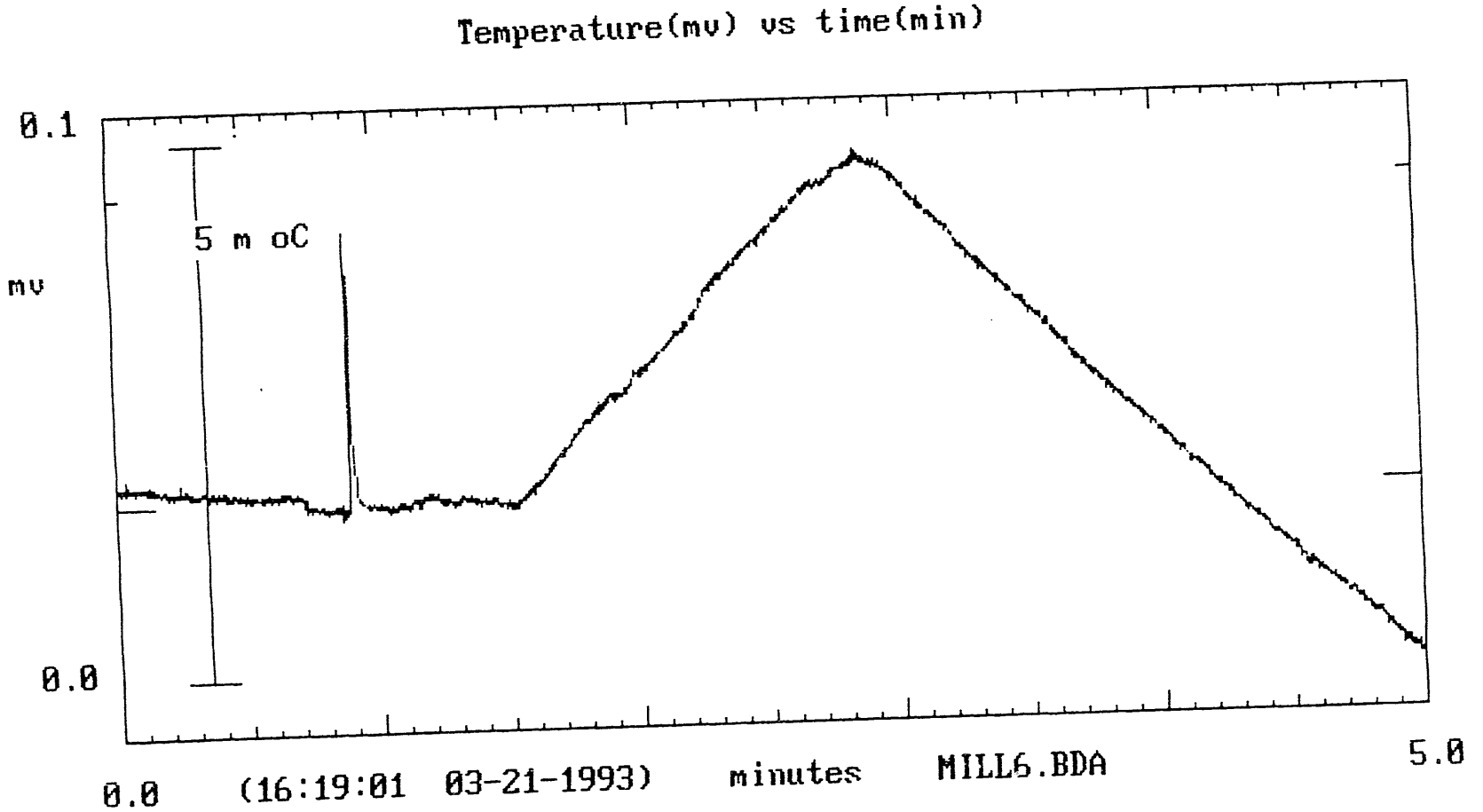
Temperature(mv) vs time(min)
0.1
5 m oC
mv
0.0
0.0
(16:19:01 03-21-1993)
minutes
MILL6.BDA
5.0

Figure 11c

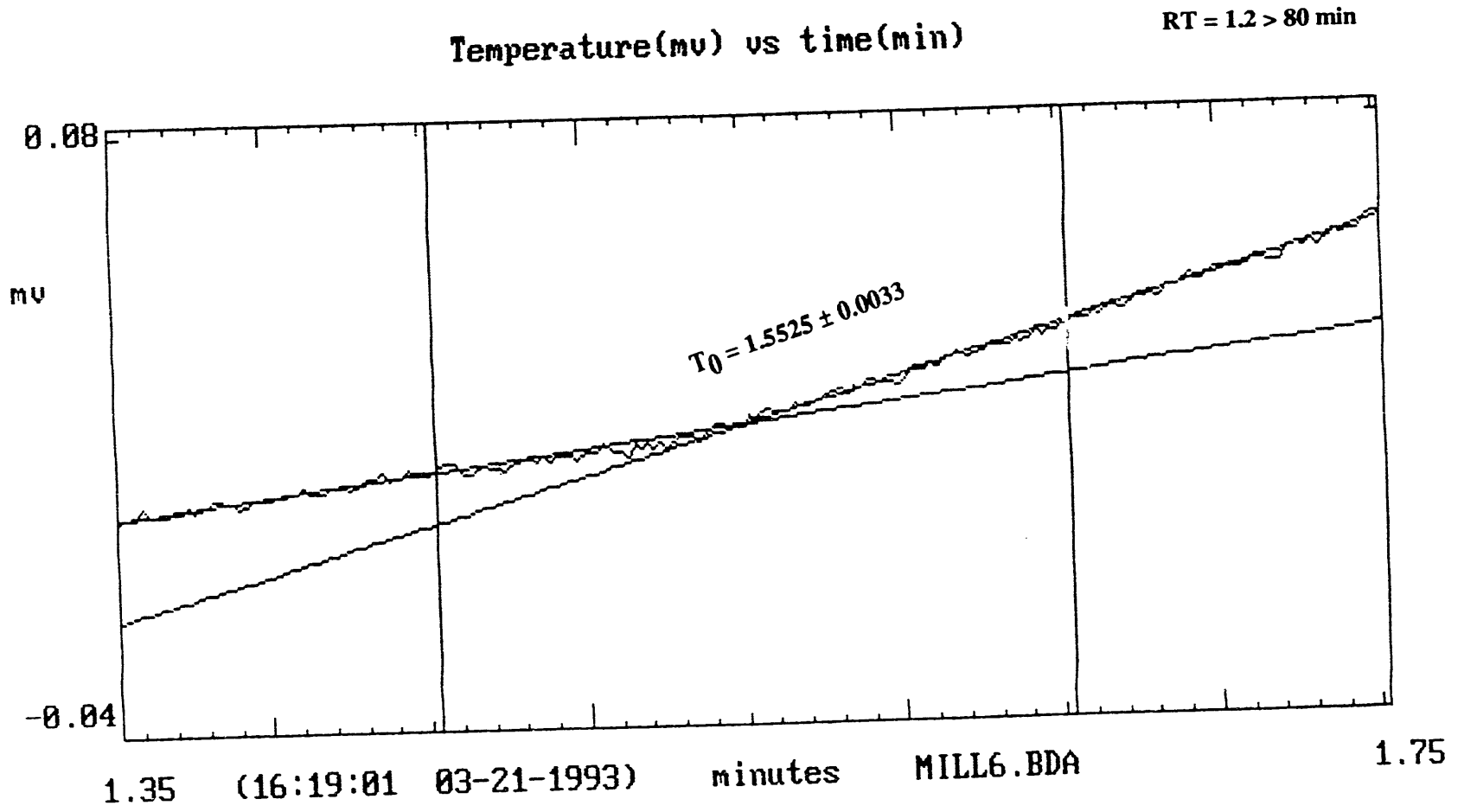
Temperature(mv) vs time(min)
RT = 1.2 > 80 min
0.08
mv
-0.04
$T_0 = 1.5525 \pm 0.0033$
1.35
(16:19:01 03-21-1993)
minutes
MILL6.BDA
1.75

Figure 11d

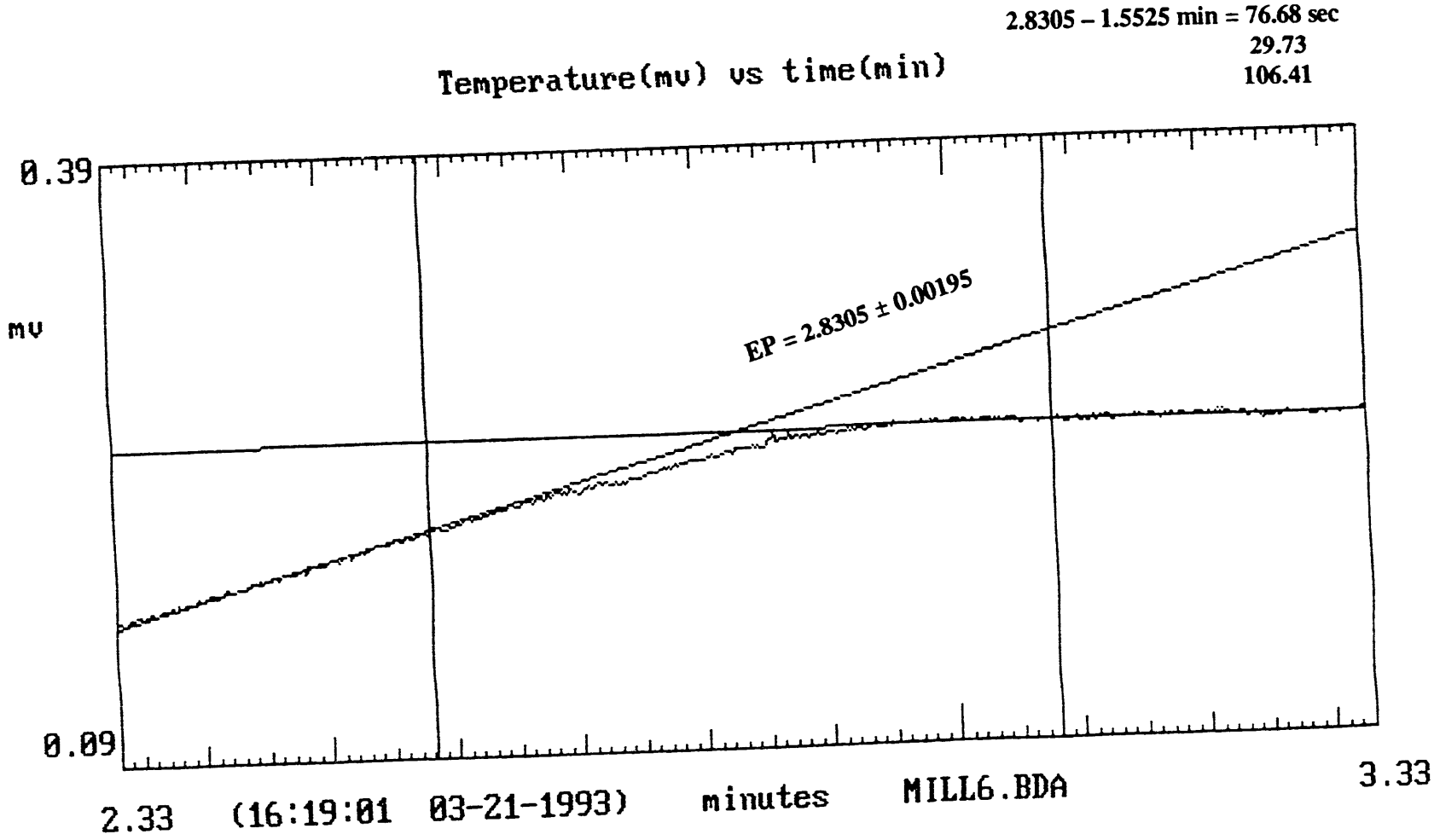
2.8305 – 1.5525 min = 76.68 sec
29.73
106.41
Temperature(mv) vs time(min)
0.39
mv
EP = 2.8305 ± 0.00195
0.09
2.33
(16:19:01 03-21-1993)
minutes
MILL6.BDA
3.33

DATE
FILMED
8/11/93
END